Photochemistry of (Fulvalene)tetracarbonyldiruthenium and Its Derivatives: Efficient Light Energy Storage Devices

Roland Boese,[1a] J. Kevin Cammack,[1b] Adam J. Matzger,[1b] Kai Pflug,[1b] William B. Tolman,[1b,c] K. Peter C. Vollhardt,*[,1b] and Timothy W. Weidman[1b]

Contribution from the Department of Chemistry, University of California at Berkeley, Chemical Sciences Division, Lawrence Berkeley National Laboratory, Berkeley, California 94720-1460, and Institut für Anorganische Chemie der Universität-Gesamthochschule, Universitätstrasse 3-5, D-45117 Essen, Germany

Received March 5, 1997[⊗]

Abstract: Broad-band irradiation (λ_{max} = 350 nm) of $FvRu_2(CO)_4$ (**1**, Fv = η^5:η^5-bicyclopentadienyl) resulted in rapid isomerization to colorless (μ_2-η^1:η^5-cyclopentadienyl)$_2Ru_4(CO)_4$ (**2**) in a novel process involving a formal dinuclear oxidative addition to a C−C bond. The product reverted to **1** upon heating in solution or in the solid state, under the latter conditions with an enthalpy change of −29.8 (1.5) kcal mol^{-1}. Mechanistic studies with a mixture of **1** and **1**-d_8 revealed the absence of label scrambling, pointing to intramolecular pathways. The quantum yield (0.15) was unaffected by the presence of CCl_4, and no chlorination products were observed under these conditions. Irradiation of solutions of **1** or **2** with 300 nm light provided Fv(μ_2-η^1:η^5-cyclopentadienyl)$_2Ru_4(CO)_6$ (**6**) or, in the presence of alkynes, the adducts $FvRu_2(CO)_3$(RCCR) (**8**−**10**, R = H, C_6H_5, CO_2CH_3). Heating **1** and PR_3 (R = CH_2CH_3, CH_3, or OCH_3) yielded $FvRu_2(CO)_3(PR_3)$ (**12**−**14**), in which a fluxional process occurs characterized by intramolecular terminal to bridging carbonyl exchange. While **12** and **13** were inert, compound **14** rapidly and reversibly afforded the $P(OCH_3)_3$-substituted analog of **2** (**15**) upon irradiation with UV light. The two diastereomeric 3,3′-di-*tert*-butyl-substituted fulvalene analogs of **1** (**19**) underwent the same reaction sequence with complete retention of stereochemistry, via the diastereomeric photoproducts **20**. A double regiochemical labeling experiment proceeded with retention of connectivity and stereochemistry. A concerted mechanism for the photoisomerization is consistent with the experimental observations, but a biradical pathway cannot be ruled out. Kinetic data for the isomerizations of **2**, **15**, **20a**, and **20b** to their respective metal−metal-bonded Fv precursors were determined. The entropies of activation (+7 to +21 eu) suggested a disordered transition state. A sequence involving reversible CO loss was ruled out through a crossover experiment with **2**-^{13}CO. Kinetic and labeling experiments point to a change in mechanism when the thermal reversion of **2** to **1** was run under CO (∼1 atm). The occurrence of ligand-induced C−C coupling was indicated through studies of the reactivity of **2** with $P(CH_3)_3$. Photoisomer **2** reacts with excess CCl_4 to give $FvRu_2(CO)_4Cl_2$) by yet another mechanism. As in the potoisomerization of **1**, the thermal reversion of **2** may follow a concerted pathway, although biradical intermediates cannot be excluded.

During the last decade, the photochemistry of dinuclear organometallic complexes has received extensive attention, in part because such structures undergo a wide variety of important reactions upon photoexcitation, including ligand substitution, disproportionation, and various redox processes.[2,3] Detailed mechanistic information concerning the primary photoprocesses, as well as the reactions of the intermediates so produced, has become available for several systems, including the dimers $Cp_2M_2(CO)_4$ (Cp = η^5-C_5H_5, M = Fe, Ru) that are structural analogs of the subject of this report.[2,4,5] Extensive studies of the iron dimer suggest that it undergoes at least three independent primary photoprocesses. These are metal−metal bond homolysis to form two mononuclear radicals, CO loss to give a paramagnetic, triply-carbonyl-bridged dinuclear species, and metal−metal bond disruption without fragmentation to afford a reactive intermediate held together by a single bridging carbonyl. Formation of the vast array of products isolated after irradiation in the presence of added reagents such as CCl_4, phosphines, or alkynes has been rationalized by invoking

⊗ Abstract published in *Advance ACS Abstracts,* July 1, 1997.

(1) (a) Universität-GH Essen. (b) University of California at Berkeley. (c) Current address: University of Minnesota, 207 Pleasant Street S.E., Minneapolis, MN 55455. (d) Current address: Applied Materials, 3225 Oakmead Village Drive, Sunnyvale, CA 95054.

(2) For reviews, see: (a) Geoffroy, G. L.; Wrighton, M. S. *Organometallic Photochemistry*; Academic Press: New York, 1979. (b) Wrighton, M. S.; Graff, J. L.; Luong, J. C.; Reichel, C. L.; Robbins, J. L. In *Reactivitiy of Metal−Metal Bonds*; Chisholm, M. H., Ed.; ACS Symposium Series 155; American Chemical Society: Washington, DC, 1981; pp 85−111. (c) Stiegman, A. E.; Tyler, D. R. *Acc. Chem. Res.* **1984**, *17*, 61. (d) Stiegman, A. E.; Tyler, D. R. *Coord. Chem. Rev.* **1985**, *63*, 217. (e) Meyer, R. J.; Caspar, J. V. *Chem. Rev.* **1985**, *85*, 187. (f) Lee, K.-W.; Hanckel, J. M.; Brown, T. L. *J. Am. Chem. Soc.* **1986**, *108*, 2266. (g) Poliakoff, M.; Weitz, E. *Adv. Organomet. Chem.* **1986**, *25*, 277. (h) Albers, M. O.; Robinson, D. J.; Singleton, E. *Coord. Chem. Rev.* **1987**, *79*, 1. (i) Baird, M. C. *Chem. Rev.* **1988**, *88*, 1217.

(3) For recent work, see, inter alia: (a) Zhang, H. T.; Brown, T. L. *J. Am. Chem. Soc.* **1993**, *115*, 107. (b) Scott, S. L.; Espenson, J. H.; Zhu, Z. *J. Am. Chem. Soc.* **1993**, *115*, 1789. (c) Knorr, J. R.; Brown, T. L. *J. Am. Chem. Soc.* **1993**, *115*, 4087. (d) Male, J. L.; Davis, H. B.; Pomeroy, R. K.; Tyler, D. R. *J. Am. Chem. Soc.* **1994**, *116*, 9353. (e) Song, X.; Brown, T. L. *Organometallics* **1995**, *14*, 1478. (f) Peters, J.; George, M. W.; Turrer, J. J. *Organometallics* **1995**, *14*, 1503.

(4) For recent studies on the Fe dimer, see: (a) McKee, S. D.; Bursten, B. E. *J. Am. Chem. Soc.* **1991**, *113*, 1210. (b) Dixon, A. J.; George, M. W.; Hughes, C.; Poliakoff, M.; Turner, J. J. *J. Am. Chem. Soc.* **1992**, *114*, 1719. (c) Zhang, S.; Brown, T. L. *J. Am. Chem. Soc.* **1992**, *114*, 2723. (d) Zhang, S.; Brown, T. L. *Organometallics* **1992**, *11*, 4166. (e) Zhang, S.; Brown, T. L. *J Am. Chem. Soc.* **1993**, *115*, 1779. (f) Kvietok, F. A.; Bursten, B. E. *J. Am. Chem. Soc.* **1994**, *116*, 9807. (g) Vitale, M.; Lee, K. K.; Hemann, C. F.; Hille, R.; Gustafson, T. L.; Bursten, B. E. *J. Am. Chem. Soc.* **1995**, *117*, 2286.

(5) For investigations of the Ru dimer, see: (a) Abrahamson, H. B.; Palazzotto, M.C.; Reichel, C. L.; Wrighton, M. S. *J. Am. Chem. Soc.* **1979**, *101*, 4123. (b) Feasey, N. D.; Forrow, N. J.; Hogarth, G.; Knox, S. A. R.; Macpherson, K. A.; Morris, M. J.; Orpen, A. G. *J. Organomet. Chem.* **1984**, *267*, C41. (c) Bloyce, P. E.; Campen, A. K.; Hooker, R. H.; Rest, A. J.; Thomas, N. R.; Bitterwolf, T. E.; Shade, J. E. *J. Chem. Soc., Dalton Trans.* **1990**, 2833.

S0002-7863(97)00706-3 CCC: $14.00 © 1997 American Chemical Society

trapping of reactive intermediates resulting from these primary photoreactions.[2−4] The detailed photochemistry of the ruthenium dimer has been less well scrutinized,[5] but the occurrence of metal−metal bond homolysis and, possibly, CO loss processes similar to those observed for the iron congener appears to be indicated.

We have been interested for some time in the utilization of the fulvalene (Fv) ligand as a matrix on which to anchor two metals in close proximity, even in the absence of an intermetallic bond, and have observed remarkable chemisty arising from such systems.[6] As part of this program and in the hope of uncovering new dinuclear transformations, an investigation of the photochemistry of $FvRu_2(CO)_4$ (**1**) was undertaken. We have discovered that, in contrast to its analog $Cp_2Ru_2(CO)_4$, **1** does not fragment upon irradiation but instead transforms in a highly unusual, thermally reversible isomerization reaction. Details of this chemistry, as well as studies of secondary photoreactions and experiments aimed at assessing the scope, stereo- and regiochemistry, and mechanism of the photoisomerization of **1** and its derivatives are described herein. Some preliminary portions of this work have been reported.[7]

Results and Discussion

Structure of $FvRu_2(CO)_4$ (1). Bright yellow crystals of **1** were isolated from the reaction of purified dihydrofulvalene with $Ru_3(CO)_{12}$ in refluxing dimethoxyethane.[7b] Although the proposed empirical formula for **1** was confirmed by elemental analysis, spectroscopic studies provided insufficient information for a definitive structural assignment. Both solid state (KBr) and solution (benzene, THF, CH_2Cl_2, and CH_3CN) IR spectra of **1** revealed two sharp terminal carbonyl absorptions, a pattern contrasting with the complex, solvent-dependent IR spectra observed for the analog $Cp_2Ru_2(CO)_4$ that contains equilibrating bridging and terminal carbonyl ligands.[5a,c] The optical absorption spectrum of **1** in THF showed a characteristic peak at λ_{max} 329 nm similar to that reported for the unbridged form of $Cp_2Ru_2(CO)_4$ (λ_{max} 330 nm).[5a,c] In addition, there is a shoulder at 388 nm tailing into the visible range, whereas the Cp dimer has a corresponding band at 435 nm. By analogy to the assignments for the absorption maxima of $Cp_2Ru_2(CO)_4$, the features exhibited by **1** can be attributed to metal−metal $\sigma \rightarrow \sigma^*$ and $d\pi \rightarrow \sigma^*$ transitions, thus implying the existence of a single bond between the ruthenium atoms. The presence of metal−metal bonding in **1** was further supported by the observation of two AA′BB′ pseudotriplets separated by ∼1.50 ppm (200 MHz, solvent-dependent) in its ^{1}H NMR spectrum, a pattern analogous to those seen for other Fv-bridged metal−metal-bonded complexes.[6,8] Although its mass spectrum lacked peaks with *m/z* values for molecular ions larger than those corresponding to a dinuclear structure, higher nuclearity formulations could not be excluded on this basis alone, because efficient fragmentation to dinuclear fragments on electron impact might have occurred. In view of the ambiguities presented by the spectroscopic data acquired for **1**, an X-ray structure determination was carried out.

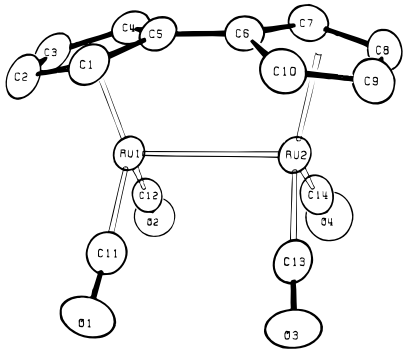

Figure 1. ORTEP diagram (50% probability surface) of **1**.

As shown by the ORTEP drawing in Figure 1, **1** contains a pair of ruthenium atoms linked by a metal−metal bond and a bridging Fv ligand, with four terminal carbonyls bound in a highly symmetrical and eclipsed array. Selected bond lengths and angles are listed in Table 1.

The molecule deviates from C_{2v} symmetry only slightly, as reflected by a minor twist around the C5−C6 axis (Cp−Ru−Ru−Cp torsion angle = 4.3°). The metals lie approximately on cyclopentadienyl centroid axes and each five-membered ring appears planar. The bend of the Fv ligand, defined as the angle between the planes of the Cp rings, is relatively large (θ = 28.5°), suggesting that the normally planar Fv moiety is strained and leading to the expectation of a longer than normal Ru−Ru single bond distance. This hypothesis is based on X-ray structural data for the series $FvM_2(CO)_6$ (M = Cr, Mo, W) in which metal−metal separations were found to be significantly greater than in the respective Cp dimers.[6a,c] Avoidance of nonbonding contacts between carbonyl ligands in addition to alleviation of strain by decreasing the Fv bend were cited to account for these lengthened bonds. Similar arguments may be applied to **1**. Thus, the Ru−Ru distance in **1** [2.821 (1) Å] is longer than that observed in $Cp_2Ru_2(CO)_4$ [2.735 (2) Å],[9] a discrepancy due in part to the inability of the carbonyl ligands in **1** to adopt a doubly-bridged arrangement because of the constraining Fv platform. The Ru−Ru separation in **1** is also greater than that reported for the bis(cyclopentadienyl)methane complex (η^5:η^5-$C_5H_4CH_2C_5H_4$)$Ru_2(CO)_4$ [2.766 (1) Å],[10] perhaps a more appropriate model because it contains exclusively terminal carbonyl ligation. In contrast to the staggered configuration of carbonyl ligands in (η^5:η^5-$C_5H_4CH_2C_5H_4$)$Ru_2(CO)_4$, however, the carbonyls in **1** are essentially eclipsed, thus preventing a closer approach of the metal atoms.

Thermally Reversible Photoisomerization of 1. Room temperature irradiation of bright yellow solutions of **1** in THF with long wavelength light (maximum intensity at 350 mn, Rayonet photochemical reactor) or simply sun light resulted in the rapid formation of a colorless photoproduct **2** in up to 80% yield (Scheme 1). Saturation of the THF solution with CO or addition of alkynes seemed to have little or no effect on the efficiency of the initial formation of **2**, new complexes (vide infra) appearing only after it became the predominant species. Both mass spectral and analytical data for **1** and **2** were identical to within experimental errors, suggesting that **2** possessed a structure isomeric with its precursor. The IR spectrum of **2** contained two carbonyl stretching bands (1960 and 2000 cm^{-1})

(6) (a) For a review, see: McGovern, P. A.; Vollhardt, K. P. C. *Synlett* **1990**, 493. (b) For a discussion of the "fulvalene concept" and leading references, see: Tilset, M.; Vollhardt, K. P. C.; Boese, R. *Organometallics* **1994**, *13*, 3146. (c) De Azevedo, C. G.; Boese, R.; Newman, D. A.; Vollhardt, K. P. C. *Organometallics* **1995**, *14*, 4980. (d) Brown, D. S.; Delville, M.-H.; Vollhardt, K. P. C.; Astruc, D. *Organometallics* **1996**, *15*, 2360. (e) Boese, R.; Bräunlich, G.; Gotteland, J.-P.; Hwang, J.-T.; Troll, C.; Vollhardt, K. P. C. *Angew. Chem., Int. Ed. Engl.* **1996**, *35*, 995. (f) McGovern, P. A.; Vollhardt, K. P. C. *J. Chem. Soc., Chem. Commun.* **1996**, 1593.

(7) (a) Vollhardt, K. P. C.; Weidman, T. W. *J. Am. Chem. Soc.* **1983**, *105*, 1676. (b) Vollhardt, K. P. C.; Weidman, T. W. *Organometallics* **1984**, *3*, 82. (c) Drage, J. S.; Tilset, M.; Vollhardt, K. P. C.; Weidman, T. W. *Organometallics* **1984**, *3*, 812. (d) Boese, R.; Tolman, W. B.; Vollhardt, K. P. C. *Organometallics* **1986**, *5*, 582.

(8) Meyerhoff, D. J.; Nunlist, R.; Tilset, M.; Vollhardt K. P. C. *Magn. Reson. Chem.* **1986**, *24*, 709.

(9) Mills, O. S.; Nice, J. P. *J. Organomet. Chem.* **1967**, *9*, 339.

(10) Knox, S. A. R.; Macpherson, K. A.; Orpen, A. G.; Rendle, M. C. *J. Chem. Soc., Dalton Trans.* **1989**, 1807.

(11) For the $\Delta H_f°$ of cyclopentadienylidene, see: McDonald, R. N.; Bianchina, E. J., Jr.; Tung, C. C. *J. Am. Chem. Soc.* **1991**, *113*, 7115.

Table 1. Selected Interatomic Distances (Å) and Angles (deg) for **1a**,[a] **2a**,[a] **6**, **8b**,[b] and **23a**[c]

distances (Å)				angles (deg)			
				1			
Ru1−Ru2	2.821(1)	Ru1−C11	1.860(3)	Ru2−Ru1−C11	94.40(8)	Ru2−Ru1−C12	93.32(7)
Ru1−C12	1.866(3)	Ru2−C13	1.870(3)	Ru2−Ru1−Cp1	105.4	C11−Ru1−C12	91.49(11)
Ru2−C14	1.886(3)	Ru1−Cp1	1.894	C11−Ru1−Cp1	130.2	C12−Ru1−Cp1	131.1
Ru2−Cp2	1.896	C5−C6	1.457(3)	Ru1−Ru2−C13	92.96(7)	Ru1−Ru2−C14	93.97(8)
C−C_{Cp}(min)	1.398(3)	C−C_{Cp}(max)	1.431(3)	Ru1−Ru2−Cp2	104.7	C13−Ru2−C14	90.50(11)
C−C_{Cp}(av)	1.416			C13−Ru2−Cp2	130.1	C14−Ru2−Cp2	132.9
				2			
Ru1−Ru1	3.456(1)	Ru1−C11	1.870(9)	Cp1−Ru1−C11	130.0	Cp1−Ru1−C12	129.3
Ru1−C12	1.849(9)	Ru1−Cp1	1.882	Cp1−Ru1−C17	106.9	C17−Ru1−C11	93.7(3)
Ru1−C17	2.077(6)	C17−C17	2.60(1)	C17−Ru1−C12	95.1(3)	C11−Ru1−C12	92.1(3)
C−C_{Cp}(min)	1.393(12)	C−C_{Cp}(max)	1.443(9)				
C−C_{Cp}(av)	1.424						
				6			
Ru1−Ru2	2.718(1)	Ru1−Ru3	2.800(1)	Ru2−Ru1−Ru3	61.16(1)	Ru2−Ru1−Cp3	135.62
Ru2−Ru3	2.808(1)	Ru1−C21	1.836(5)	Ru3−Ru1−Cp3	123.30	Ru1−Ru2−Ru3	60.85(1)
Ru1−C22	2.003(5)	Ru2−C22	2.039(5)	Ru1−Ru2−Cp2	138.13	Ru3−Ru2−Cp2	108.10
Ru2−C23	1.855(5)	Ru3−C24	1.828(5)	C22−Ru2−Cp2	116.72	C23−Ru2−Cp2	132.10
Ru4−C25	1.858(6)	Ru4−C26	1.878(6)	Ru1−Ru3−Ru2	58.00(1)	Ru1−Ru3−Cp1	137.45
Ru4−C11	2.082(4)	Ru3−C16	2.096(4)	Ru2−Ru3−Cp1	101.88	C16−Ru3−Cp1	110.33
Ru3−Cp1	1.915	Ru2−Cp2	1.896	C24−Ru3−Cp1	130.02	C11−Ru4−Cp4	118.54
Ru1−Cp3	1.915	Ru4−Cp4	1.900	C25−Ru4−Cp4	128.39	C26−Ru4−Cp4	126.59
C5−C6	1.451(7)	C−C_{Cp}(min)	1.390(7)	Ru2−C22−Ru1	84.5(2)		
C−C_{Cp}(max)	1.439(8)	C−C_{Cp}(av)	1.415				
				8			
Ru1−Ru2	2.719(1)	Ru1−C11	1.862(3)	Ru2−Ru1−C11	119.11(7)	Ru2−Ru1−C13	48.66(8)
Ru1−C13	2.035(3)	Ru1−C14	2.095(3)	Ru2−Ru1−C11	69.60(9)	Ru2−Ru1−Cp1	106.7
Ru1−Cp1	1.903	Ru2−C12	1.854(3)	C11−Ru1−C13	86.30(10)	C11−Ru1−C14	84.00(10)
Ru2−C13	2.055(3)	Ru2−C15	2.089(3)	Cp1−Ru1−C11	133.7	Cp1−Ru1−C13	122.8
Ru2−Cp2	1.915	C14−C15	1.268(4)	Cp1−Ru1−C14	119.9	Ru1−Ru2−C12	117.12(8)
C5−C6	1.443(4)	C−C_{Cp}(min)	1.387(4)	Ru1−Ru2−C13	48.03(7)	Ru1−Ru2−C15	69.83(7)
C−C_{Cp}(max)	1.445(4)	C−C_{Cp}(av)	1.411	Ru1−Ru2−Cp2	106.2	C12−Ru2−C13	83.39(11)
				C12−Ru2−C15	85.06(11)	Cp2−Ru2−C12	136.0
				Cp2−Ru2−C13	123.7	Cp2−Ru2−C15	118.7
				Ru1−C13−Ru2	83.31(9)	Ru1−C14−C15	110.3(2)
				Ru2−C15−C14	110.3(2)		
				23a			
Ru1−Ru2	3.462(1)	Ru1−C11	1.878(5)	CP1−Ru1−C6	107.6	Cp1−Ru1−C11	130.4
Ru1−C12	1.875(5)	Ru2−C13	1.846(4)	Cp1−Ru1−C12	131.7	Cp2−Ru2−P	127.0
Ru2−P	2.222(1)	Ru1−C6	2.076(5)	Cp2−Ru2−C13	132.9	Cp2−Ru2−Cl	107.7
Ru2−Cl	2.080(5)	C1−C6	2.639(7)	C6−Ru1−C11	93.2(2)	C6−Ru1−C12	91.9(2)
Ru1−Cp1	1.896	Ru2−Cp2	1.898	C1−Ru2−C13	94.3(2)	C1−Ru2−P	93.8(1)
C−C_{Cp}(min)	1.386(7)	C−C_{Cp}(max)	1.452(8)	C11−Ru1−C12	90.4(2)	C13−Ru2−P	91.1(2)
C−C_{Cp}(av)	1.429						

[a] Details of the structural determination have been published as Supplementary Material in ref 7a. [b] Details of the structural determination have been published as Supplementary Material in ref 7c. [c] Cp stands for the centroid of the ligand.

shifted only slightly from those of **1** (1952 and 2020 cm^{-1}), indicating a similarly symmetric disposition of carbonyl ligands in both complexes. The ^1H NMR spectrum of photoproduct **2** revealed the AA′BB′ pseudotriplet pattern typical for monosubstituted Cp rings, but the decreased chemical shift difference between the two signals compared to **1** (0.71 vs 1.50 ppm at 200 MHz) suggested that **2** lacked a metal−metal bond.[8] This conclusion was supported by the electronic absorption spectrum, which, in contrast to that of **1**, only exhibited broad features with λ_{max} below 300 nm. Finally, an upfield shift of the less-intense quaternary signal of the three peaks observed in the $^{13}C\{^1H\}$ NMR spectrum of **2** from the analogous signal in the spectrum of **1** (from 94.4 to 85.8 ppm) indicated a change in the bonding of the ruthenium atoms to the Cp rings. Since we were unable to discern the structure of the photoproduct **2** from the above spectroscopic and analytical data, an X-ray structure determination was performed.

Surprisingly, considering the estimated robust nature of the Cp−Cp linkage in fulvalene itself and the inertness of the former in the chemistry of Fv dimetals,[6,7] the X-ray diffraction experiment revealed that photolysis of **1** had caused it to rearrange to a compound lacking both a metal−metal bond and a C−C bond between the Cp rings (Figure 2). The unit cell for crystalline **2** contains two independent molecules with local C_{2h} symmetry, with the Ru atoms in each molecule attached to two terminal carbonyl ligands, to one Cp ring in an η^5 manner, and to the other Cp via a single bond.

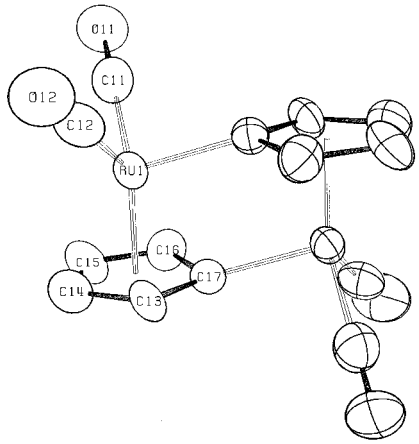

Figure 2. ORTEP diagram (50% probability surface) of one of the molecules of **2** in the unit cell.

Scheme 1

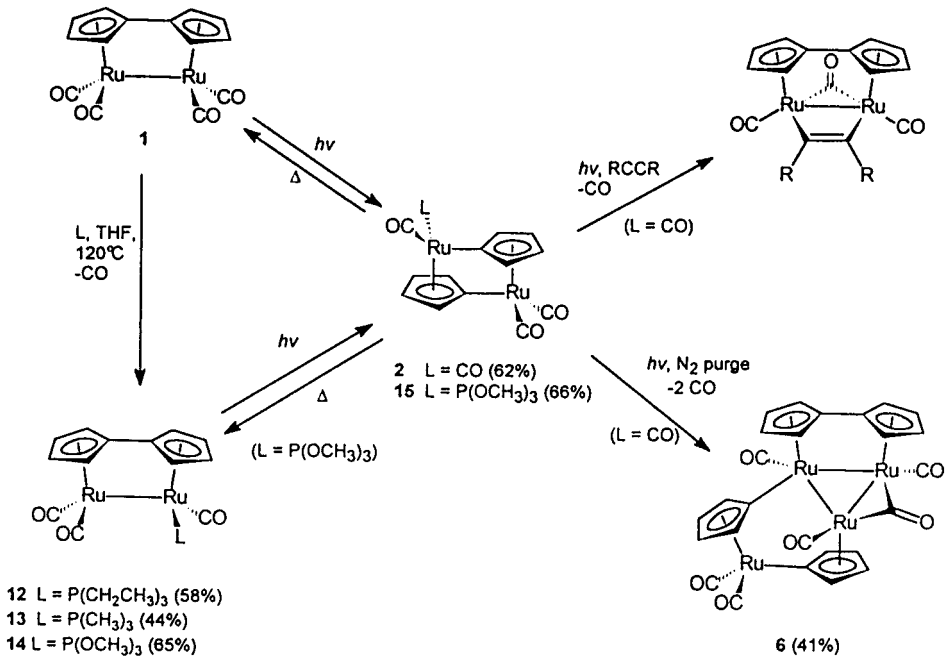

Selected bond distances and angles are listed in Table 1. Significant bonding interactions between the two Ru atoms or between the cyclopentadienylidene carbons are ruled out by the respective distances (averaged over both molecules) 3.47 and 2.64 Å. The Cp rings are planar, the respective σ-bonded metals being located 0.58 Å out of plane, presumably in order to attain coordination geometries only minimally distorted from a normal three-legged piano stool.

The Ru atoms reside on the centroid axis of their respective π-bound Cp's, arguing against a significant contribution of resonance formulation **3** to the structure of **2**. Indeed, the average Ru−C σ bond distance (2.09 Å) is similar to those reported for other ruthenium C_{sp^2} single bonds[12,19d] and is significantly larger than those in ruthenium carbenes (∼1.8−1.9 A).[13] Alkylidene carbons on ruthenium have also been

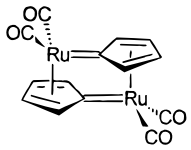

3

reported to exhibit ^{13}C NMR resonances at ∼250 ppm,[13] much further downfield than the corresponding signal observed for **2**, which exhibits a chemical shift (96.8 ppm) that is in agreement with model systems.[14]

Even more remarkable than the photoinduced dinuclear oxidative addition reaction of **1** that produced **2** is its facile thermal reversal. This process occurred at moderate temperatures (>65 °C) in solution, allowing for the ready recording of kinetic data (vide infra). It also occurred in the crystal, white **2** transforming to yellow **1** at 208 °C without loss of crystallinity, impressive considering the profound topological change involved.[15] Differential scanning calorimetry of the process revealed a sharp exotherm at 208 °C associated with an enthalpy release of −29.8 (1.5) kcal mol^{-1} followed by a lesser endotherm at 288 °C, signalling the melting point of **1**. Amusingly, the apparent changes in mechanical stress associated with this solid state rearrangement causes crystals of **2** to jump several centimeters high when heated to 208 °C on a hot plate, a phenomenon described in the literature as "thermosalient"[16a] or "Hüpfeffekt".[16b] The efficiency and cleanliness (10 cycles were performed without any apparent decomposition) of the **1**/**2** system (and its derivatives) suggest potential utility as a photochemical energy storage device. While organic molecules have been extensively investigated in this regard, organometallic examples are rare.[18]

Mechanistically, the interconversion **1** ⇌ **2** poses an intriguing problem, as it involves the cleavage of both the metal−metal and Cp−Cp bonds and their respective reconnections to η^1-C_5H_4-M units. Metal−metal bond rupture is, of course, precedented by the analogous homolysis of $Cp_2Ru_2(CO)_4$,[5] but the oxidative addition to the central fulvalene bond has fewer analogies in the literature. For example, while there are a number of reports on the (occasionally reversible) conversion of an η^5-Cp to a μ_2-η^1:η^5-Cp ligand, these involve Cp−H "activation".[19] Such activation, particularly starting with early metallocene derivatives, may proceed, often through the intermediacy of dimers $[(\eta^1{:}\eta^5\text{-}C_5H_4)(\eta^5\text{-}C_5H_5ML]_2$, structurally related to **2**, directly or in a stepwise manner, but generally irreversibly, to the corresponding fulvalene dimetals (i.e., analogs of **1**).[20] There are only two other reported cases of

(12) (a) Heineke, D.; Vahrenkamp, H. *Angew. Chem., Int. Ed. Engl.* **1993**, *32*, 1048. (b) Arce, A. J.; De Sanctis, Y.; Manzur, J.; Capparelli, M. V. *Angew. Chem., Int. Ed. Engl.* **1994**, *33*, 2193. (c) Arce, A. J.; De Sanctis, Y.; Machado, R.; Manzur, J.; Capparelli, M. V. *Organometallics* **1996**, *15*, 1834.

(13) Roper, W. R. In *Advances in Metal Carbene Chemistry*; Schubert, U., Ed.; Kluwer Academic Press: Dordrecht, The Netherlands, 1989; p 27.

(14) Herberhold, M.; Feger, W.; Kölle, U. *J. Organomet. Chem.* **1992**, *436*, 333.

(15) *Organic Solid State Chemistry*; Desiraju, G. R., Ed.; Elsevier: New York, 1987.

(16) (a) Gigg, J.; Gigg, R.; Payne, S.; Conant, R. *J. Chem. Soc., Perkin Trans. 1* **1987**, 2411. (b) Kohne, B.; Praefcke, K.; Mann, G. *Chimia* **1988**, *42*, 139.

(17) (a) *Photochromism, Molecules and Systems*; Dürr, H., Bouas-Laurent, H., Eds.; Elsevier: New York, 1990. (b) *Organic Photochromes*; El'tsov, A. V., Ed.; Consultants Bureau: New York, 1990.

(18) For example, see: Adams, R. D.; Cortopassi, J. E.; Aust, J.; Myrick, M. *J. Am. Chem. Soc.* **1993**, *115*, 8877.

(19) For recent work, see: (a) Alvarez, M. A.; García, M. E.; Riera, V.; Ruiz, M. A.; Bois, C.; Jeannin, Y. *J. Am. Chem. Soc.* **1995**, *117*, 1324. (b) Rigny, S.; Leblanc, J.-C.; Moïse, C.; Nuber, B. *J. Chem. Soc., Chem. Commun.* **1995**, 45. (c) Nakajima, T.; Mise, T.; Shimizu, I.; Wakatsuki, Y. *Organometallics* **1995**, *14*, 5598. (d) Bitterwolf, T. E.; Shade, J. E.; Hansen, J. A.; Rheingold, A. L. *J. Organomet. Chem.* **1996**, *514*, 13.

Scheme 2

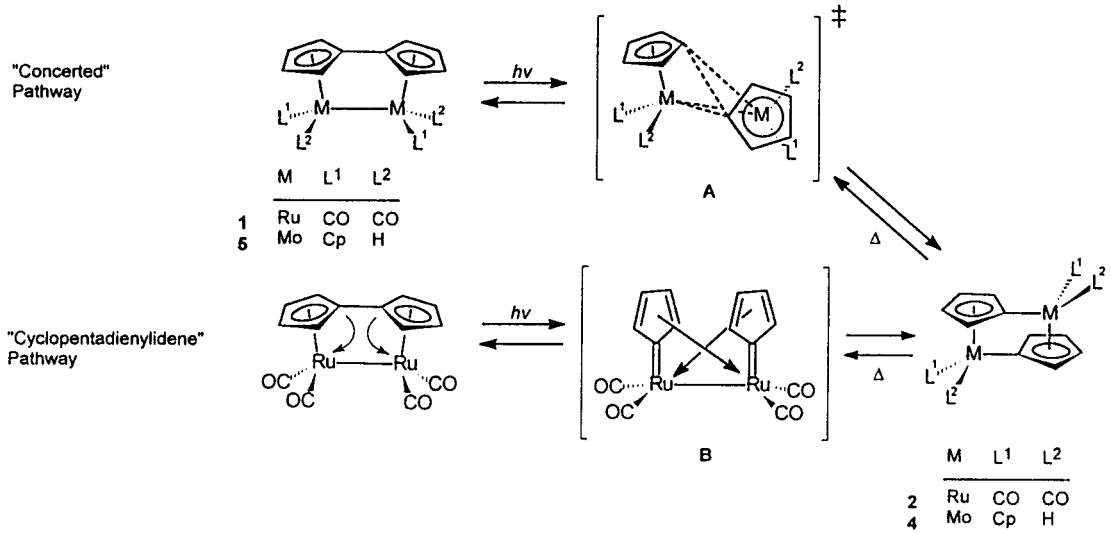

reversible-ligating Fv to $(\eta^1{:}\eta^5\text{-Cp})_2$ interconversions. One is purely thermal, involves Zr as the metal, and is driven in either direction by external phosphine association−dissociation.[21] The second represents the closest analogy to our system and is based on the hydridomolybdenocene dimer.[22] In this investigation, **4** was observed to convert to **5** on heating, a process that retroceded on irradiation (Scheme 2). A plausible, but experimentally not proven, concerted mechanism was invoked featuring a tetrahedral transition state **A** common to both processes and reminiscent of that pictured for a $\pi 2s + \pi 2a$ cycloaddition of two ethenes.[23] However, the presence of the hydride ligands allows for the formulation of alternative pathways through the reversible generation of η^5-CpM fragments.

Secondary Photoprocesses: Cluster Formation and Photosubstitution. Extended irradiation of THF solutions of **1** and/or its rapidly formed photoisomer **2** in quartz vessels with broadband UV light ($\lambda_{max} = 300$ nm) under a slow purge of N_2 yielded a new purple complex (**6**, Scheme 1). A dimeric formulation for **6** containing two Fv liands, two ruthenium atoms, and a total of six carbonyl ligands was suggested by the combined mass spectral and analytical data. Specifically, its chemical ionization mass spectrum exhibited a parent ion at *m/z* 828 corresponding to dimerization of **1** or **2** with loss of two carbonyls. A complex structure for **6** was implied by its infrared spectrum, which contained several terminal and bridging carbonyl ligand absorptions. This hypothesis was confirmed by the ^{1}H NMR spectrum, which contained a total of 16 distinct resonances of equal integration between 6.0 and 3.4 ppm, pointing to the presence of at least four C_5H_4 ligands in a completely unsymmetrical environment.

An X-ray crystal structural analysis provided the unambiguous structural assignment illustrated by the ORTEP drawing in Figure 3. The molecule contains a metal−metal-bonded triruthenium core connected unsymmetrically to the fourth Ru center via $\eta^1{:}\eta^5$-C_5H_4 bridges. All bond distances and angles (cf. Table 1) appear normal, and each Ru atom may be attributed an 18-electron configuration. Overall, the structure might be viewed as being formally derived from addition of a Ru atom in **1** to a Ru-η5-Cp bond in **2**. Interestingly, prolonged thermolysis[24] or photolysis[5b,25] of $Cp_2Ru_2(CO)_4$ furnishes a number of tri-, tetra-, and pentanuclear clusters. Under the latter conditions, two systems resulting from "Cp−H activation" are obtained, one of which (**7**)[5b] could be regarded as a rearranged dihydro analog of **6** with its center unit (within the dashed box) representing a "trapped" transition state for the interconversion of **1** to **2** (Scheme 2).

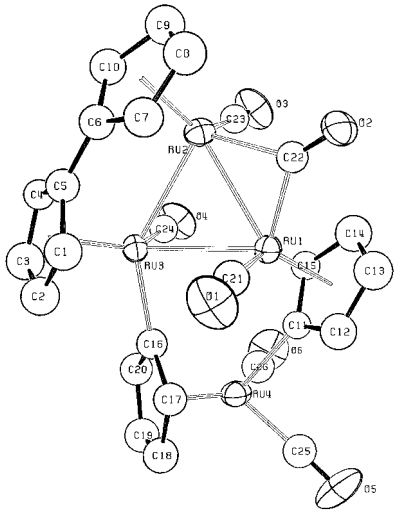

Figure 3. ORTEP diagram (50% probability surface) of **6**.

Results of experiments aimed at pinpointing the source of **6** are listed in Table 2. Consideration of entries 2, 4, and 5 reveals that the cluster is formed far more efficiently starting from pure **2** than from **1** or a 5:1 mixture of **2:1** (previously prepared by photolysis with 350 nm light in the absence of an N_2 purge). The presence of CO diminished the rate of conversion to **6** (entries 1 and 3). A possible rationalization of these results is that (i) photoactivation of **2**, rather than **1**, is responsible for formation of **6** and (ii) a decarbonylation of **2**[26] that is inhibited

(20) For recent work, see: (a) Wielstra, Y.; Gambarotta, S.; Meetsma, A.; deBoer, J. L. *Organometallics* **1989**, *8*, 250. (b) Wielstra, Y.; Gambarotta, S.; Meetsma, A.; Spek, A. L. *Organometallics* **1989**, *8*, 2948. (c) Hiller, J.; Thewalt, U.; Polášek, M.; Petrusová, L.; Varga, V.; Sedmera, P.; Mach, K. *Organometallics* **1996**, *15*, 3752. (d) Varga, V.; Mach, K.; Polášek, M.; Sedmera, P.; Hiller, J.; Thewalt, U.; Troyanev, S. I. *J. Organomet. Chem.* **1996**, *506*, 241.

(21) Wielstra, Y.; Gambarotta, S.; Spek, A. L.; Smeets, W. J. J. *Organometallics* **1990**, *9*, 2142.

(22) (a) Berry, M.; Cooper, N. J.; Green, M. L. H.; Simpson, S. J. *J. Chem. Soc., Dalton Trans.* **1980**, 29. (b) Barral, M. C.; Green, M. L. H.; Jimenez, R. *J. Chem. Soc., Dalton Trans.* **1982**, 2495. (c) Green, M. L. H.; Mtetwa, V. S. B.; Sella, A.; Chernega, A. N. *J. Chem. Soc., Dalton Trans.* **1994**, 201.

(23) Lowry, T. H.; Richardson, K. S. *Mechanism and Theory in Organic Chemistry*, 3rd ed.; Harper and Row: New York, 1987; p 912.

(24) (a) Blackmore, T.; Cotton, J. D.; Bruce, M. I.; Stone, F. G. A. *J. Chem. Soc. A* **1968**, 2931. (b) Knox, S. A. R.; Morris, M. J. *J. Chem. Soc., Dalton Trans.* **1987**, 2087.

(25) Dyke, A. F.; Knox, S. A. R.; Naish, P. J.; Taylor, G. E. *J. Chem. Soc., Dalton Trans.* **1982**, 1297.

Table 2. Comparison of the Photoreactivity of **1** and **2** at 300 nm

entry	composition of starting mixture[a]	reaction time (min)	product composition after photolysis (%)[b]			
			1	**2**	**6**	**8**
1	**1**/CO (1 atm)	5	78	22	<2	
		15	36	64	<2	
		30	23	77	<2	
2	**1**/N_2	5	78	22	<2	
		15	33	63	4	
		30	16	77	7	
3	**2**/CO (1 atm)	5	3	93	4	
		15	5	90	5	
		30	11	85	4	
4	**2**/N_2	5	2	84	16	
		15	4	73	23	
		30	7	65	28	
5	**1** + **2** (1:5)/N_2	5	18	78	4	
		15	16	76	8	
		30	13	77	10	
6	**1**/ethyne (satd)	5	76	24		<2
		15	31	63		6
		30	15	74		11
7	**2**/ethyne (satd)	5	<2	81		19
		15	3	68		29
		30	5	55		41

[a] Total concentration of metal complexes was 0.001 M in each case (THF solvent, ambient temperature). [b] Determined by inegration of ^{1}H NMR spectra.

by added CO lies along the reaction route. The reduced yields

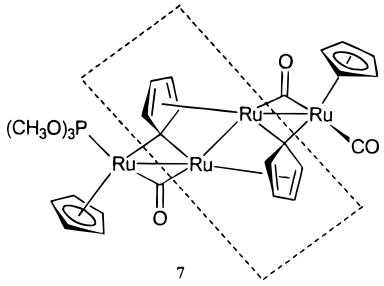

7

of **6** observed when starting from a 5:1 mixture of **2:1** would then be due to light absorption by **1**, which essentially acts as a filter. Indeed, **1** absorbs light considerably more efficiently than **2** in the pertinent region of the electronic spectrum. Of course, the data, while noteworthy, do not rule out initial CO loss from **1** by a relatively higher energy photoprocess independent of isomerization, resulting in a reactive 16-electron fragment that could then attack the Ru-η^5-Cp bond of **2** to give **6**. In this scenario, efficient formation of **6** might only result when trapping reagent **2** was in excess, consistent with the findings summarized in Table 2. Slow thermal (vide infra) or photochemical reversion of **2** to **1** at ambient temperature could account for intervention of the latter even when pure **2** is used as starting material (entry 4). In this instance, the higher concentration of **2** present in the reaction mixture would allow more efficient trapping of the CO loss intermediate, thus resulting in relatively higher conversion to **6**. Whatever the mechanism of cluster formation, rearrangement of **1** is clearly the most facile photochemical reaction, as **6** appeared only after **2** became predominant in the reaction mixtures.

In solutions saturated with ethyne, irradiation of **1** again gave **2** initially, followed by slow conversion to an orange product **8** (Scheme 1). The mass spectrum of **8** displayed a molecular ion peak at *m/z* 440, consistent with the occurrence of exchange of carbonyl ligand for ethyne. Partly symmetrical incorporation

(26) See, for example, a detailed study of the near UV photoejection of CO from $CpRu(CO)_2CH_3$: Kazlauskas, R. J.; Wrighton, M. S. *Organometallics* **1982**, *1*, 602.

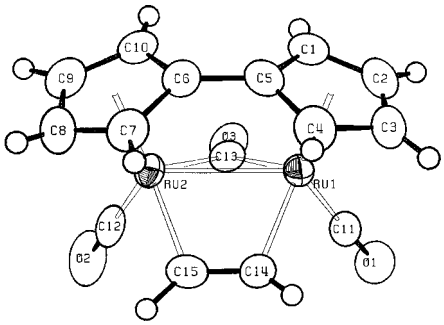

Figure 4. ORTEP diagram (50% probability surface) of **8**.

of the latter was indicated by the presence of four Fv resonances and one peak due to the ethyne protons in the ^{1}H NMR spectrum. The bridging formulation **8** was supported by the IR spectrum, in which both terminal and bridging carbonyl absorptions were evident.

A rigorous assignment of the diruthenacyclobutene structure **8** rested on an X-ray crystallographic analysis. The relatively rare parallel alkyne bonding mode[27] is illustrated by the ORTEP drawing in Figure 4 (bond distances and angles are listed in Table 1). The new ligand is bound symmetrically with a C−C distance of 1.268(4) Å, intermediate between ethene (1.337 Å) and ethyne (1.204 Å). Similar diruthenium alkyne complexes are known.[2h,10,28] Presumably because of the presence of multiple bridging ligands, the Fv bend angle of 31.6° is larger and the metal−metal bond distance of 2.719(1) Å shorter than the corresponding values for **1**.

Irradiation of **1** in the presence of diphenylethyne or dimethyl 2-butynedioate yielded adducts which, on the basis of elemental analyses and the similarity of their ^{1}H NMR and IR spectra with those of **8**, were identified as relatives **9** and **10**, respectively (Scheme 1). No evidence was present for the generation of fulvalene diruthenacyclopentenones analogous to **11**, obtained upon photolysis of $Cp_2Ru_2(CO)_4$ in the presence of alkynes.[2h]

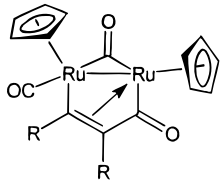

11

Similar to the synthesis of cluster **6**, irradiation of solutions of pure **2** yielded **8** far more rapidly than those of **1** under identical conditions (Table 2, entries 6 and 7), pointing to decarbonylation of **2** as the primary photoprocess leading to **8**, although other pathways are conceivable (vide infra).

Syntheses, Dynamic Behavior, and Photoreactions of $FvRu_2(CO)_3L$ (L = Phosphine or Phosphite). The syntheses of monosubstituted phosphine-containing complexes were attempted in order to probe the electronic and, to some extent, the steric requirements of the photoisomerization of **1** to **2**. The compounds $FvRu_2(CO)_3L$ **12**−**14** (Scheme 1) were prepared by the treatment of **1** with an excess of the respective phosphine

(27) For a discussion of the various ways in which alkynes may be attached to metal clusters, see: Adams, R. D. *Chem. Soc. Rev.* **1994**, 335 and references cited therein.

(28) For recent examples, see, inter alia: (a) Colborn, R. E.; Dyke, A. F.; Gracey, B. P.; Knox, S. A. R.; Macpherson, K. A.; Mead, K. A.; Orpen, A. G. *J. Chem. Soc., Dalton Trans.* **1990**, 761. (b) Omori, H.; Suzuki, H.; Kakigano, T.; Moro-oka, Y. *Organometallics* **1992**, *11*, 989. (c) Field, J. S.; Haines, R. J.; Sundermeyer, J.; Woollan, S. F. *J. Chem. Soc., Dalton Trans.* **1993**, 3749. (d) Mirza, H. A.; Vittal, J. J.; Puddephatt, R. J. *Organometallics* **1994**, *13*, 3063.

Scheme 3

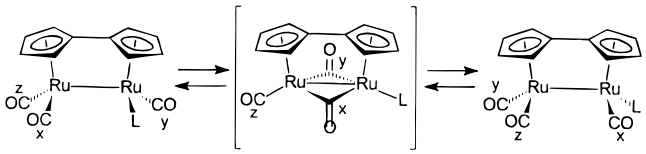

or phosphite in THF at elevated temperature (120 °C, sealed vessel). Yields of **12** were somewhat variable because of the occurrence of competing Fv slippage reactions (vide infra).[7d] Treatment of **1** with an excess of PPh_3 for 1 week at 120 °C gave only starting material (>95%).

The formulations of **12**−**14** as monosubstituted derivatives of **1** are based on their combined analytical and spectral data. All displayed three terminal carbonyl absorptions in their IR spectra and a singlet with the expected chemical shift in their $^{31}P\{^1H\}$ NMR spectra. At room temperature, ^1H NMR spectroscopy revealed the appropriate signals for the hydrogens on the respective phosphine ligands, but in the Fv region only four broad signals instead of the expected eight were seen. At higher temperatures, these signals sharpened, while cooling caused increased broadening and, for some, splitting into separate peaks.

This behavior can be interpreted as being due to a fluxional process which leads to intrametallic site exchange of the phosphine ligand (Scheme 3). A possible mechanism that accounts for such a movement involves pairwise shifts of two carbonyl ligands from terminal to bridging positions as observed for numerous Cp metal carbonyl dimers,[29] including those of Ru.[2h,5] An important consequence of this pathway is the restriction of intermetallic migration to only two of the carbonyls (**x** and **y**, Scheme 3) while the third (**z**) is expected to remain not only terminally bound but also in a position opposite to the phosphine with respect to a molecular plane bisecting the molecule along the π system. As a result, in the ^{13}C NMR spectra of **12**−**14**, carbonyls **x** and **y** should give rise to a singlet and a doublet (with J_{CP}) at the low-temperature limit and to a doublet (with $J = 0.5\ J_{CP}$) at high temperature, while the signal for carbonyl **z** should remain a singlet throughout.

These predictions were confirmed by acquisition of variable temperature (−75 °C to +55 °C) ^{13}C NMR data for ^{13}CO-labeled **12**, prepared via treatment of ^{13}CO-labeled **1** (vide infra) with $P(CH_2CH_3)_3$. Simulation and line shape analysis[30] of the four spin system allowed calculation of the activation parameters: $\Delta G^{\ddagger}_{298} = 12.0(1)$ kcal mol^{-1}, $\Delta H^{\ddagger} = 8.8(2)$ kcal mol^{-1}, and $\Delta S^{\ddagger} = -10.6$ (1.0) eu. Of note is the negative entropy of activation, consistent with the presence of the proposed constrained, doubly-carbonyl-bridged transition state leading to the proposed intermediate in Scheme 3.

The electronic influence of the phosphine ligands is clearly reflected in the UV−vis absorption maxima of **12**−**14** (compared to **1** in Table 3). While there appears to be only a small perturbation of what is presumed to be the $\sigma \rightarrow \sigma^*$ band on going from the poorer [L = CO or $P(OCH_3)_3$; **1** and **14**] to the stronger [L = $P(CH_2CH_3)_3$ or $P(CH_3)_3$; **12** and **13**] donor ligands, there is a significant shift of the $d\pi \rightarrow \sigma^*$ band to longer wavelengths. The latter is to be expected, since a strong donor ligand would be predicted to cause the metal $d\pi$ orbitals to rise in energy, thus decreasing the $d\pi \rightarrow \sigma^*$ energy gap. Differences in the photochemical reactivity of **12**−**14** parallel this trend.

Table 3. UV−Vis Absorption Maxima for $FvRu_2(CO)_3L$ in THF

compound	L	$\sigma \rightarrow \sigma^*$, nm ($\epsilon$)	$d\pi \rightarrow \sigma^*$, nm ($\epsilon$)
12	$P(CH_2CH_3)_3$	338 (6300)	460 (1200)
13	$P(CH_3)_3$	333 (8700)	444 (1260)
14	$P(OCH_3)_3$	333 (7400)	418 (1100)
1	CO	333 (7100)	388 (sh, 1500)

When solutions of trialkylphosphine derivatives **12** and **13** in THF were irradiated (λ_{max} = 350 nm), gradual darkening and formation of an insoluble precipitate took place. Only traces of numerous Fv-containing products were detectable by ^1H NMR spectroscopy even after 20 h. Attempts to trap possible intermediates by photolysis in the presence of CCl_4 were unsuccessful.

In contrast, irradiation of **14** cleanly and rapidly afforded the colorless photoisomer **15** (Scheme 1). Its asymmetry is reflected in the ^1H NMR spectrum, which exhibits eight multiplets in the Fv hydrogen region. Appropriate signals for ligated $P(OCH_3)_3$ are apparent in the ^1H and $^{31}P\{^1H\}$ NMR spectra, and the IR spectrum contains three absorptions in the terminal carbonyl region. Mass spectral and analytical data confirm that **15** is indeed an isomer of **14**. In addition, the UV−vis absorption spectrum of **15** is virtually superimposable with that of tetracarbonyl analog **2**. Like **2**, photoproduct **15** reverted cleanly to its metal−metal-bonded isomer **14** upon heating in solution. An attempt to effect this isomerization in the solid state was foiled by the melting of **15** (mp 82−83 °C) prior to reaction.

It is difficult to provide reasons for the observed differences in photochemistry between the trialkylphosphine complexes **12** and **13** and the phosphite and tetracarbonyl complexes **14** and **1**, respectively, without the benefit of a detailed theoretical framework.[31] It may be that the failure of the former species to photoisomerize has an electronic rather than steric origin, since $P(CH_3)_3$ and $P(OCH_3)_3$ are similar in size (cone angles are 118° and 107°, respectively),[32] yet very different in their electron-donating capabilities.[33] This statement must be viewed with caution, however, for although these differences are reflected by shifts in the $d\pi \rightarrow \sigma^*$ absorption band in the UV−vis spectra of the complexes, all four systems exhibit similar maxima for the $\sigma \rightarrow \sigma^*$ feature. It is important to note also that a number of other FvM_2L_x complexes prepared by us[6a,b,34] do not visibly enter the **1** ⇌ **2** manifold equivalent.

Mechanistic Studies of the Thermally Reversible Photorearrangement. The highly unusual nature of the dinuclear oxidative addition−reductive elimination processes inherent in the reactions that interconvert **1** and **2** and their respective phosphite-substituted analogs, combined with the potential applicability of the systems to light energy storage technology, provided great incentive to undertake extensive mechanistic studies.

(a) Crossover Experiment. An obvious photoisomerization pathway for **1** would be dissociation into mononuclear fragments and their subsequent recombination to **2**. A possible structure for such fragments is suggested by the literature, in which $(Cp)_3ThR$ was postulated to evolve RH on heating to generate

(29) (a) Cotton, F. A.; Wilkinson, G. *Advanced Inorganic Chemistry*, 5th ed.; Wiley: New York, 1988; p 1325. (b) Lukehart, C. M. *Fundamental Transition Metal Organometallic Chemistry*; Brooks/Cole: Monterey, CA, 1985. (c) For a recent reference, see: Chen, X.; Mann, B. E. *Organometallics* **1996**, *15*, 3703.

(30) Line shape analysis was performed at the UCB Computer Center using DYNAMAR, a modified version of a program developed by Meakin, P.; Muetterties, E. L.; Tebbe, F. N.; Jesson, J. P. *J. Am. Chem. Soc.* **1971**, *93*, 4701 and Jesson, J. P.; Meakin, P. *Acc. Chem. Res.* **1973**, *6*, 269. Data were plotted according to the Eyring equation $\ln(nhk/k_bT) = -\Delta H^{\ddagger}/RT + \Delta S^{\ddagger}/R$ and fitted to a straight line using linear least-squares program ACTPAR, altered from the original of Binsch, G.; Kessler, H. *Angew. Chem., Int. Ed. Engl.* **1980**, *19*, 411.

(31) (a) Veillard, A.; Dedieu, A. *Nouv. J. Chim.* **1983**, 683. (b) Sevin, A.; Hengtai, Y.; Chaquin, P. *J. Organomet. Chem.* **1984**, *262*, 391.

(32) Tolman, C. A. *Chem. Rev.* **1977**, *77*, 313.

(33) (a) Tolman, C. A. *J. Am. Chem. Soc.* **1970**, *92*, 2953. (b) Rahman, M. M.; Liu, H.-Y.; Eriks, K.; Prock, A.; Giering, W. P. *Organometallics* **1989**, *8*, 1.

(34) Drage, J. S.; Kahn, A. P.; McGovern, P.; Myrabo, R. L.; Tilset, M.; Vollhardt, K. P. C.; Weidman, T. W. Unpublished results.

Table 4. Average Quantum Yields of the Photoreactions of **1** and $Cp_2Ru_2(CO)_4$[a]

reaction medium[b]	$Cp_2Ru_2(CO)_4 \rightarrow 2CpRu(CO)_2Cl$[c]	**1** → **2**[c]
acetone-d_6		0.14
acetone-d_6, 1.0 M CCl_4	0.39	0.15
benzene-d_6		0.17
benzene-d_6, 1.0 M CCl_4	0.47	0.15
THF-d_8		0.15
THF-d_8, 1.0 M CCl_4	0.37	0.14
THF-d_8, CO (1 atm)		0.13

[a] All irradiations performed with 350 ± 20 nm lamps using a rotating stage in a Rayonet reactor at an average intensity of 2.8×10^{-6} photons min^{-1}, as determined by ferrioxalate actinometry. Conversions to product were measured using ^1H NMR spectroscopy and are reported as disappearance quantum yields. [b] Solution concentrations were 2.0×10^{-3} M in starting material. [c] Estimated standard deviation: ±15%.

intermediate (cyclopentadienylidene)Cp_2Th, which dimerized to the thorium analog of **2**.[35] In order to test this hypothesis, a crossover experiment was performed. A deuterated dihydrofulvalene solution was prepared as in the synthesis of **1** but starting with 95% deuterated cyclopentadiene[36] and performing the aqueous extraction step using D_2O. Reaction with $Ru_3(CO)_{12}$ gave **1**-d_8 (~90% label by ^1H NMR spectroscopy). A diglyme solution containing an equimolar mixture of **1** and **1**-d_8 was then subjected to the sequence irradiation−heating three times. Analysis of mass spectral data obtained before and after this treatment revealed the absence of any crossover of the label, clearly ruling out a dissociative or other mechanism allowing for intermolecular scrambling.

(b) Quantum Yield Measurements. The quantum efficiency of the photoisomerization process using broad band irradiation (λ_{max} = 350 nm, 325−375 nm range) was determined using ferrioxalate actinometry to approximate the photon flux and quantitative ^1H NMR spectroscopy to assess the conversion of **1** to **2**. In addition, parallel measurements of the photooxidation of $Cp_2Ru_2(CO)_4$ to $CpRu(CO)_2Cl$ in solvent mixtures containing CCl_4 provided the opportunity to compare relative efficiencies of photoisomerization and of halide abstraction and to assure consistency of the quantum yield values with those previously reported for $Cp_2Ru_2(CO)_4$.[5a]

The results listed in Table 4 reveal an average quantum efficiency for photoisomerization of **1** of 0.15(3) and a lack of dependence on the reaction media. Most significant were the results of photolysis performed in the presence of CCl_4. Chlorinated products were not observed, at least on the time scales of the experiments (vide infra) and quantum yields for rearrangement of **1** to **2** were unaffected by the presence of the radical trap. In contrast, and in general agreement with previous reports,[5a] irradiation of $Cp_2Ru_2(CO)_4$ under identical conditions produced $CpRu(CO)_2Cl$ with quantum yields for the disappearance of starting material ranging from 0.37 to 0.47.

The efficient production of halogenated monomer from $Cp_2Ru_2(CO)_4$ has been attributed to metal−metal bond cleavage to give two 17-electron $CpRu(CO)_2$ radicals during the primary photoprocess.[5a] Decarbonylation has also been identified as an initial photochemical event in related iron systems.[4] Direct analogy to the photochemistry observed for $Cp_2M_2(CO)_4$ (M = Fe, Ru) would therefore suggest either metal−metal bond homolysis ("biradical" mechanism, vide infra) or CO loss (perhaps into a solvent cage) as possible primary steps in the photoisomerization of **1** to **2**. The first alternative would afford biradical intermediate **16**, while the second would result in the formation of a coordinatively unsaturated species of possible structure **17**. Either intermediate might be trapped by CCl_4 (or

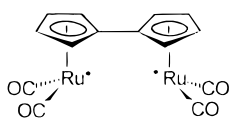

16

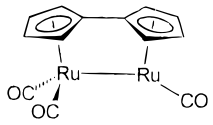

17

other two electron ligands).[2] The absence of chlorination products [or simple (vide infra) exchange in the presence of external ligands (e.g., ^{13}CO) suggests that either **16** or **17** are not formed or that their conversion to **2** takes place relatively fast.[19d] Thus, their expected reactivity as coordinatively unsaturated complexes may be considerably attenuated by delocalization through the Fv π system.[6,7,37] In any case, the divergent photochemical reactivity of the Fv-bridged vs $(CpM)_2$ molecules in the presence of CCl_4 provides clear evidence for unique reactivity enabled by the Fv ligand.

(c) Stereo- and Regiochemistry of the Interconversion of 1 and 2. Regardless of the nature of the initial species generated on photoexcitation of **1**, the details by which the subsequent remarkable reorganization to **2** occurs are difficult to envision. One mechanistic possibility is a "concerted" pathway analogous to that postulated by Green for the dimolybdenum system **4**/**5** (Scheme 2).[22] Alternatively, a dimeric version **B** of (cyclopentadienylidene)$Ru_2(CO)_2$ ("cyclopentadienylidene" pathway, Scheme 2) can be suggested. Differences in the topological changes associated with these "concerted" and "cyclopentadienylidene" pathways are apparent. In the latter, π-bound ligands trade places with the metals (i.e., each Fv bridgehead carbon becomes σ-bonded to the Ru to which it was initially attached in a π sense), while in the former they do not (each bridgehead carbon forms a σ bond with the opposite Ru atom). More importantly, a consequence of the "cyclopentadienylidene" route is the emergence of both Cp rings complexed to the ligand face opposite to that encountered in starting material (i.e., inversion of stereochemistry), a feature absent in the "concerted" mechanism (retention). The recognition of this potential stereochemical aspect of the interconversion of **1** and **2** forces one to consider the possibility that other (unspecified) mechanisms may be in operation, causing inversion or retention at one or both of the rings. Stereochemical tests can be used to probe these questions and, in addition, to assess differences between the mechanisms for the thermal- and light-induced reactions, repectively, a procedure analogous to that used to validate the Woodward−Hoffmann rules.[38]

Specifically, introduction of substituents on the Fv ligand of **1** results in the presence of stereogenic metal centers, thus allowing, in principle, the distinction of reaction pathways that involve either inversion or retention. For simplicity and in a preliminary attempt to shed some light on these mechanistic possibilities, the symmetrical ligand 3,3′-di-*tert*-butylfulvalene was chosen, accessible in its complexed form from its dihydroderivative **18** (Scheme 4).[39] Slow addition of purified dissolved **18** to a boiling solution of $Ru_3(CO)_{12}$ in DME and subsequent column chromatography gave a 35% yield of a 1:1 mixture of the bright yellow diastereomers **19a** and **19b**, which were separated by HPLC. As expected, the products had very similar physical properties, but they could be differentiated on the basis of their ^1H and $^{13}C\{^1H\}$ NMR spectra. Five Fv and

(35) Baker, E. C.; Raymond, K. N.; Marks, T. J.; Wachter, W. A. *J. Am. Chem. Soc.* **1974**, *96*, 7586.

(36) McLean, S.; Webster, C. J.; Rutherford, R. J. D. *Can. J. Chem.* **1969**, *47*, 1557.

(37) (a) For a review, see: Geiger, W. E.; Connelly, N. G. *Adv. Organomet. Chem.* **1985**, *24*, 87. (b) For recent work, see: Atwood, C. G.; Geiger, W. E.; Rheingold, A. L. *J. Am. Chem. Soc.* **1993**, *115*, 5310.

(38) Woodward, R. B.; Hoffmann, R. *Angew. Chem., Int. Ed. Engl.* **1969**, *8*, 781.

(39) Brand, R.; Krimmer, H. P.; Lindner, H. J.; Hafner, K. *Tetrahedron Lett.* **1982**, *23*, 5131.

Scheme 4

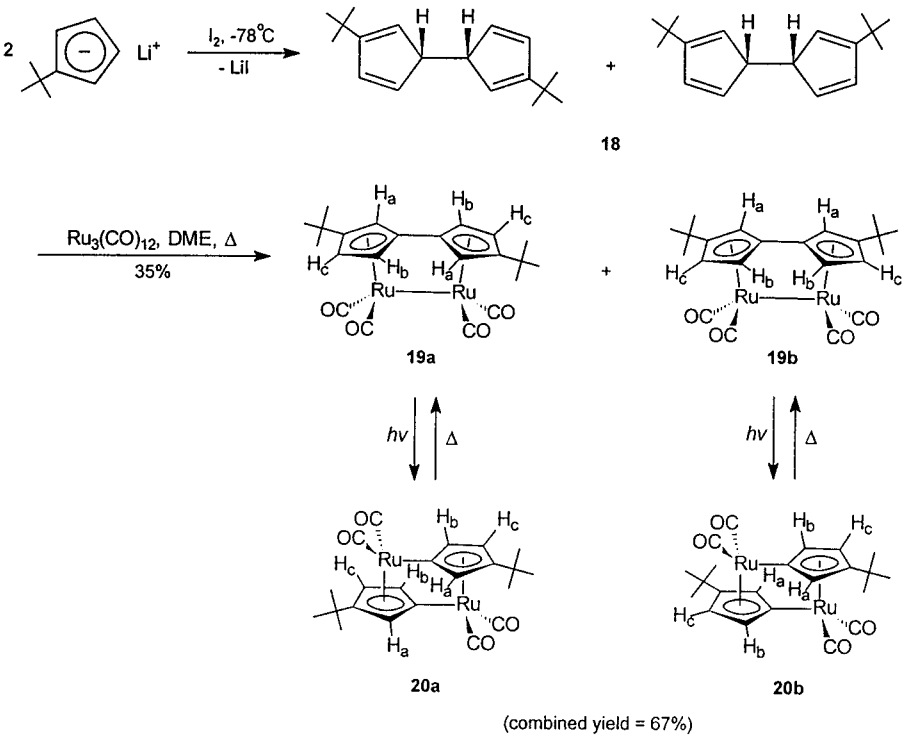

Table 5. ^{1}H−^{1}H NOE Enhancements in **19a** and **19b**[a]

hydrogen irradiated	hydrogens exhibiting enhanced signals	
	19a	**19b**
CH_3	H_a, H_c	H_a, H_c
H_a	H_b	
H_b	H_a, H_c	H_c
H_c	H_b	H_b

[a] Labeling scheme shown in Scheme 4.

two *tert*-butyl carbon peaks at the expected chemical shifts were apparent in the respective carbon spectra of both isomers. For each compound, the observation of two resonances due to the diastereotopic carbonyl carbons at room temperature indicated that, in comparison to the phosphine and phosphite derivatives **12**−**14** (and, by inference, **1**), intramolecular carbonyl exchange is slow. In their ^{1}H NMR spectra, both **19a** and **19b** exhibited an upfield singlet for the *tert*-butyl groups and three downfield doublet of doublets for the Fv hydrogens. The assignments of the latter signals and, most importantly, of the correct stereochemistry to the diastereomers were based on their characteristic relative chemical shifts and coupling constants in conjunction with ^{1}H−^{1}H NOE difference spectra. Because of its large chemical shift relative to the other two signals (e.g., δ 5.57 vs 3.74 and 3.85 ppm for **19b**), the lowest field resonance was attributed to the hydrogens β to the ring juncture for both diastereomers (H_c), an assignment consistent with previously reported data for Fv-bridged metal−metal-bonded compounds.[6−8] Of the remaining peaks, that at lower field exhibited small and equal couplings (J = 1.9 Hz) in the range expected for ^4J values in complexed five-membered rings,[40] providing compelling evidence that it arose from H_a. The ^{1}H-^{1}H NOE enhancements observed for both diastereomers are summarized in Table 5. In particular, irradiation at the resonance frequency of the hydrogens of the *tert*-butyl methyl groups allowed the highest field Fv signal in both diastereomers to be assigned to H_b, which, like H_c, exhibited both large (^3J = 2.8 Hz) and small (^4J = 1.9 Hz) couplings. Finally, the stereochemistry of both compounds was deduced from the observation of an enhancement for the signal for H_a upon irradiation of H_b (and vice versa) for **19a**, a phenomenon absent for **19b**.

The electronic absorption spectra of both diastereomers were essentially identical to that of **1**, and gratifyingly, irradiation of a 1:1 mixture of **19a** and **19b** afforded a colorless solid which, on the basis of mass spectral, analytical, and ^{1}H NMR data and the similarities between its UV−vis and IR spectra to those of **2**, was identified as a 1:1 mixture of the photoisomers **20a** and **20b** (Scheme 4). Most significantly, irradiation of pure **19a** stereospecifically gave **20a** only, while **19b** yielded solely **20b**.

The structural formulations shown for photoisomers **20a** and **20b** were derived from similar data to those obtained for their respective metal−metal-bonded precursors. ^{1}H NMR spectra of the former exhibited the expected three Fv signals, the chemical shift differences between the distinct low-field signal to the other two (δ 5.51 vs 4.86 and 4.62 ppm for **20a**; δ 5.53 vs 4.83 and 4.65 ppm for **20b**) being smaller than in **19a** and **19b**. The central absorption was attributed to H_a because of the presence of small and equal couplings (^4J = 1.8 Hz). Corroboration of this assignment as well as those of the other Fv hydrogen resonances was obtained by ^{1}H−^{1}H NOE difference spectroscopy. Of the data collected, the most important was the small (∼5%) but unambiguous enhancement of the peak due to H_a upon irradiation at the resonance frequency of H_b in **20b** and the absence of such an effect in **20a**, thus confirming the proposed stereochemistry of these photoproducts.

The thermal reactions of photoisomers **20a** and **20b** were also found to be stereospecific. Thus, heating **20a** in solution yielded only **19a**, while **20b** reverted only to **19b**. Unlike parent photoisomer **2**, solid samples of both **20a** and **20b** melted first (at 115 °C and 160 °C, respectively) and then gradually transformed into their respective yellow metal−metal-bonded precursors.

In sum, the di-*tert*-butyl-substituted analogs of **1** and **2** interconverted with strict stereospecificity. As a result, mechanisms involving stereorandomization or single inversion can be ruled out conclusively. However, routes involving either

(40) (a) Crecely, R. W.; Crecely, K. M.; Goldstein, J. H. *Inorg. Chem.* **1969**, *8*, 252. (b) Kamezawa, N. *J. Magn. Reson.* **1973**, *11*, 88.

Scheme 5

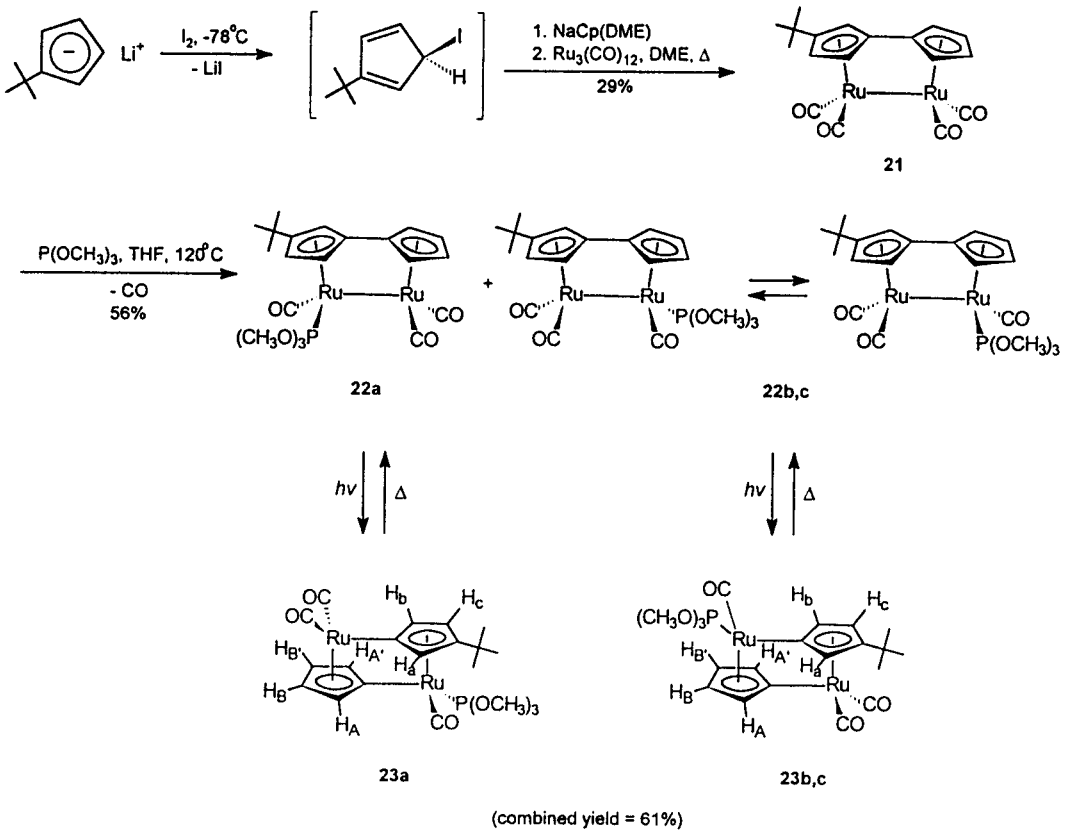

double (i.e., at both Cp's) inversion or double retention are still possible, and so are both pathways in Scheme 2.

In order to gain further information about the topological features of the photoreaction and its thermal reverse, a double-labeling experiment was devised aimed at addressing the possibility that the initial connectivity of the individual metal−ligand units was altered. This task required the preparation of substituted derivatives of **1** containing singly-labeled Fv *and* metal moieties. *tert*-Butyl was chosen as a label of the former and $P(OCH_3)_3$ for the latter, as these perturbations did not appear to alter the photoreactivity of **24** and **14**, respectively.

Addition of an equimolar amount of iodine to lithium *tert*-butylcyclopentadienide[41] at low temperature gave a solution of (presumed) 5-iodo-2-*tert*-butyl-1,3-cyclopentadiene.[42] Subsequent addition of NaCp, warming, rapid aqueous extraction, and slow addition to a solution of $Ru_3(CO)_{12}$ in boiling DME gave a crude mixture which contained **21** as the major Fv-containing product (Scheme 5). Traces of **1**, **19a**, and **19b** were removed by chromatography, and pure **21** was obtained in modest yield (29%, unoptimized) as a yellow powder. Its spectral and analytical data were consistent with the proposed structure (see Experimental Section). Treatment of **21** with $P(OCH_3)_3$ at 120 °C for 40 h cleanly afforded the monophosphite-substituted derivatives **22a**−**c** as a 1:1.3:1.3 mixture (Scheme 5). Direct chromatographic separation of these complexes proved to be troublesome, necessitating an indirect procedure for their purification through the intermediacy of the corresponding mixture of photoisomers **23a**−**c**. HPLC of the latter allowed isolation of two fractions, one containing pure **23a** and the other consisting of **23b** and **c** (1:1). On standing at room temperature in acetone-d_6 for one day, the respective products transformed cleanly and regiospecifically (^{1}H NMR) to **22a** (from **23a**) and **22b**,**c** (from **23b**,**c**). Conversely, photolysis of solutions of **22a** in THF afforded only **23a**; no **23b**,**c** was detected by ^{1}H or ^{31}P-{^{1}H} NMR spectroscopy. Similarly, irradiation of **22b**,**c** yielded only **23b**,**c**.

The gross compositions of all of these compounds were supported by mass spectral and analytical data. Within the metal−metal-bonded series **22a**−**c**, almost identical IR and UV−vis spectra were recorded, in contrast to the quite distinct NMR patterns. Thus, at room temperature, the ^{1}H NMR spectrum of the major products **22b**,**c** contained broad Fv hydrogen peaks, a sharp singlet for the *tert*-butyl substituents, and a doublet due to the phosphite methyls. Several of the ^{13}C-{^{1}H} NMR spectral lines were also broadened at this temperature and only one resonance was apparent in the ^{31}P{^{1}H} NMR spectrum. In contrast, at −70 °C 14 Fv hydrogen peaks, two singlets for the *tert*-butyl groups, and two doublets due to the phosphite nuclei emerged. Similarly, 20 Fv carbon signals, as well as the expected corresponding number of *tert*-butyl and $P(OCH_3)_3$ resonances, could be discerned in the ^{13}C{^{1}H} NMR spectrum, while ^{31}P{^{1}H} NMR spectroscopy allowed the detection of two different phosphorus centers.

These measurements are in accord with the formulation of **22b**,**c** as a mixture of diastereomers that rapidly interconvert on the NMR time scale via terminal to bridged carbonyl exchange as described above for **12**−**14** and not by intermetallic movement of the phosphite ligand. Approximate activation parameters for the process were obtained by line shape analysis[30] of variable temperature (−5 to +15 °C) ^{31}P{^{1}H} NMR spectra: $\Delta G^{\ddagger}_{298}$ = 14 (1) kcal mol^{-1}, $\Delta H^{\ddagger}$ = 15.4 (8) kcal mol^{-1}, and $\Delta S^{\ddagger}$ = 4 (5) eu.

In stark contrast to those of **22b**,**c**, NMR spectra of **22a** presented sharp peaks at temperatures as low as −70 °C. Seven resonances for the Fv hydrogens, a doublet due to the phosphite methyls, and a singlet for the *tert*-butyl group were recorded by ^{1}H NMR spectroscopy, while there were 13 signals in its ^{13}C{^{1}H} NMR spectrum. Confirmation of the proposed regio-

(41) Howie, R. A.; McQuillan, G. P.; Thompson, D. W.; Lock, G. A. *J. Organomet. Chem.* **1986**, *303*, 213.

(42) 5-Iodo-1,3-cyclopentadiene has been prepared in similar fashion: Breslow, R.; Hoffman, J. M., Jr. *J. Am. Chem. Soc.* **1972**, *94*, 2110.

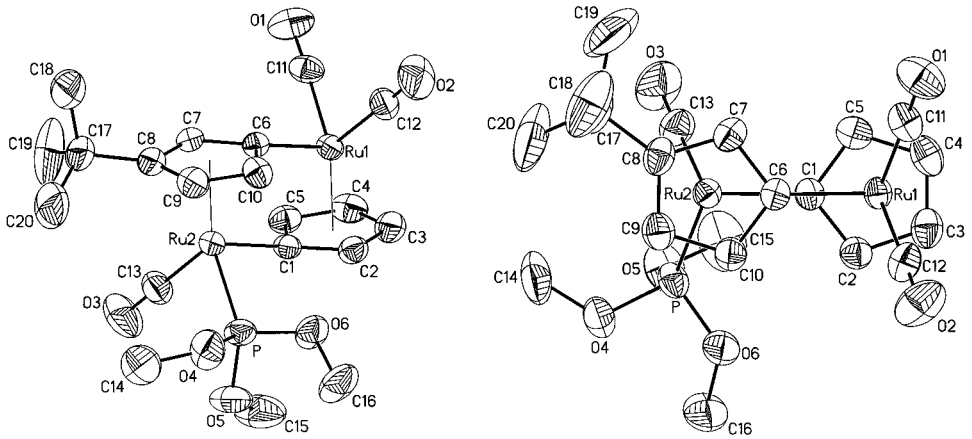

Figure 5. SHELXTL diagram of two views of **23a**.

and stereochemistry indicated in the formulation for **22a** shown in Scheme 5 was obtained from ^{1}H−^{1}H COSY and NOE difference spectra. The former allowed differentiation of the three correlated signals due to the hydrogens on the *tert*-butyl-substituted ring (H_a, H_b, and H_c) from the four resonances arising from those on the unsubstituted ring (H_A, $H_{A'}$, H_B, and $H_{B'}$). Thus identified, the peaks due to H_{a-c} were then assigned by exploiting NOE techniques similar to those applied to **19** (Table 5). In addition, irradiation at the resonance frequency of the doublet due to the phosphite methyl groups caused significant (∼10%) enhancement of the signal due to H_b and a smaller but noticeable increase of the intensity of the peak associated with H_c, as well as one of the unsubstituted ring hydrogens (presumably H_A), thus placing the phosphite ligand underneath H_b. This geometry and the apparent absence of solution fluxional behavior for **22a** may both have their origin in prohibitive steric repulsion between the *tert*-butyl group and the phosphite group.

Whereas the conversions of **23a**−**c** to **22a**−**c** were regiospecific at room temperature in acetone, heating the individual isomers **23a** or **23b**,**c** to 80−120 °C in THF or toluene gave identical mixtures of **22a**−**c** (ratio 1:1.3:1.3), suggesting thermal equilibration of the products. This suspicion was confirmed by exposing **22a** or **22b**,**c** to the same temperatures. The mechanism of this isomerization was not investigated, but it is worthy of note that it is neither mediated by light nor triggered during the ambient temperature reassembly of **22** from **23**.

The photoisomers **23a**−**c** are colorless and exhibited UV−vis absorption spectra identical to those observed for their analogs (e.g. **2**, **15**, and **20**). Identification of the major fraction as a 1:1 mixture of the diastereomers **23b** and **23c** was made possible by the observation of 14 multiplets for the μ_2-η^1:η^5-Cp ligands, two singlets due to the *tert*-butyl groups, and two doublets for the phosphite hydrogens in their ^{1}H NMR spectrum. The appropriate number of carbon peaks were present in the ^{13}C{^{1}H} NMR, and two singlets appeared in the ^{31}P{^{1}H} NMR spectra. Attempts to separate these diastereomers by HPLC were unsuccessful.

Compound **23a** exhibited seven signals in the Cp region of its ^{1}H NMR spectrum, 10 peaks for the ring nuclei in its ^{31}P-{^{1}H} NMR spectrum, and one singlet in its ^{31}P{^{1}H} NMR spectrum. ^{1}H−^{1}H COSY and NOE difference spectroscopy measurements gave similar results to those found for **20a**, except that the NOE enhancements of the signals due to the nuclei on the *tert*-butyl-substituted ring upon irradiation at the resonance frequency of the phosphite methyls were too small to be definitive (<5%). In order to conclusively verify the structure of this complex and, by inference, those of its isomers, an X-ray crystallographic analysis was performed.

Two views of the molecule are shown as SHELXTL drawings in Figure 5, and selected bond lengths and angles are listed in Table 1. In most respects, the structure of **23a** is remarkably similar to that of **2**. The Rul−Ru2 and C1−C6 distances in the former [3.462(1) and 2.639(7) Å, respectively] are nearly identical to those in the latter [3.456(1) and 2.596(13) Å] and indicate little or no bonding interactions between the respective sets of nuclei. The five-membered rings are planar, and each Ru atom lies along a Cp centroid axis.

Table 6. Eyring Activation Parameters (Std Deviations) Calculated for the Thermal Isomerizations of **2**, **15**, **20a**, and **20b**

starting material	product	solvent	$\Delta H^{\ddagger}$ (kcal mol^{-1})	$\Delta S^{\ddagger}$ (eu)
2	**1**	diglyme	29.9(2)	+17(2)
15	**14**	diglyme	27.6(5)	+7(1)
20a	**19a**	diglyme	31.6(1.0)	+21(2)
		decane	31.0(1.0)	+19(2)
20b	**19b**	diglyme	31.5(1.0)	+21(2)

Most important for the purposes of the double-labeling experiment, the structural data clearly establish that the phosphite ligand is attached to the Ru atom π bonded to the *tert*-butyl-substituted Cp ring in **23a**, the same arrangement that was determined via NMR methods for its metal−metal-bonded precursor **22a**. Therefore, the topological alteration inherent in the "cyclopentadienylidene" mechanism (Scheme 2) does not occur in either the photoisomerization of this system or its reverse, the connectivity of the CpM units being preserved. On the other hand, the results are certainly consistent with a "concerted" pathway.

(d) Kinetics of the Thermal Isomerizations of 2 and Its Derivatives and the Effect of Added Ligands. Solution kinetic data for the isomerizations of **2**, **15**, **20a**, and **20b** to their respective metal−metal-bonded Fv relatives were collected between 65 and 99 °C in diglyme. The solubility imparted on **20a** by the presence of *tert*-butyl groups allowed a similar determination in the nonpolar solvent decane. The extent of reaction in each case was monitored by following the increase in intensity of the electronic absorption of the product at 418 nm (see Experimental Section). Clean first-order kinetics were observed at all temperatures over greater than three half-lives, furnishing the Eyring activation parameters listed in Table 6.

The enthalpy of activation for the isomerization was generally invariant, the average value being +30 kcal mol^{-1}. The $\Delta S^{\ddagger}$ value was (except for **15**) surprisingly large and positive, +(17−21) eu. These data contain additional information with which to address the most probable mechanism of at least the thermal reversal part of the **1** ⇌ **2** manifold. In particular, they provide the impetus to delineate the relative merits of a concerted process vs rate-determining homolytic, heterolytic, and CO dissociative events, discussed in that order in the following. The possibility of the former, tantamount to the thermal reverse of what appears

to be the most attractive (but not proven) pathway for the photoisomerization of **1** (Scheme 2), would invoke a "loose" transition state connecting the two correspondingly relatively rigid ground state structures.[46] The slightly lesser $\Delta S^{\ddagger}$ value in the case of **15** might then be (vaguely) ascribed to the relative bulk of the phosphite ligand and its effect on the order of the activated complex.

While, in the absence of pertinent bond strength data, simple initial homolytic cleavage of a Ru−C σ bond followed by a rapid rearrangement to **16** and ring closure ("biradical" mechanism) cannot be ruled out, it appears unlikely on consideration of literature data which suggest a $DH°(\mathrm{Ru-C_{sp^2}})$ closer to 40 kcal mol^{-1} or more.[43,44] Moreover, a crude thermochemical estimate of bond strengths, assuming $DH°(\mathrm{Ru-C_{sp^2}}) = 30$ kcal mol^{-1} for **2** (from the above $\Delta H^{\ddagger}$ for **2** → **1**), $DH°(\mathrm{Ru-Ru}) \approx$ 35 kcal mol^{-1} {a value extrapolated for $[(\eta^5\text{-}C_5H_5)\mathrm{Ru(CO)_2}]_2$ from measured data for related $(\mathrm{CpM})_2$ complexes},[45] and the enthalpy change (**2** → **1**) ∼ −30 kcal mol^{-1} (vide supra), would provide a Cp−Cp bond strength of ∼55 kcal mol^{-1}, intuitively unreasonably low.[11] On the other hand, the positive and, except for **15**, large $\Delta S^{\ddagger}$ values indicate substantial disorder in the transition state, certainly consistent with a biradical pathway.[46] In principle, the latter could become evident by trapping of the potential intermediates (e.g., **16**) with CCl_4 as chlorinated products, although a negative outcome of such an experiment may be rendered inconclusive (as in the discussion of the photoisomerization of **1**, vide supra) by arguments invoking relatively short lifetimes and/or low reactivities for such species (e.g., **16**).[6,7,19d,37] In the event, exposure of **2** to rigorously purified CCl_4 in varying concentrations gave results indicative of a *change in mechanism* by which **2** is transformed. Thus, the rate of disappearance of **2** increased noticeably compared to that observed in the absence of CCl_4 [e.g., $t_{1/2}$ (dioxane, 80 °C) = 48 min; $t_{1/2}$ (dioxane, 6 equiv of CCl_4, 80 °C) = 10.8 min]. Moreover, at low concentration of the latter (ca. 1−3 equiv), complex uncharacterizable mixtures of varying composition were obtained. Only with excess (large) CCl_4 (6−96 equiv) did a clean reaction occur, the product being $\mathrm{FvRu_2(CO)_4Cl_2}$ {and not $[(\eta^5\text{-}\mathrm{ClC_5H_4})\mathrm{Ru(CO)_2}]_2$ or $(\eta^5\text{-}\mathrm{ClC_5H_4})\mathrm{Ru(CO)_2Cl}$}, rigorously identified by an alternate synthesis from **1** and $FeCl_3 \cdot 6H_2O$ and by an X-ray structural analysis (see Supporting Information). A preliminary kinetic study under pseudo-first-order (in **2**) conditions revealed an order of 0.31 with respect to CCl_4, suggesting the operation of a radical chain process, perhaps initiated by electron transfer,[47,48] followed by fast rearrangement to **16** and its subsequent chlorination. Thus, the argument against a biradical pathway from **2** to **1** rests, at present, solely on estimates for bond strengths.

The option of heterolytic metal−carbon rupture can be considered but is rendered improbable by the essential absence of any effect of changing the solvent polarity (tested on **20a**, diglyme vs decane) on the activation parameters. Direct attack by these solvents is similarly ruled out.

Last, rate-determining CO loss,[49] followed by fast rearrangement to **17** and CO recombination, remains a compelling alternative, in particular when considering the kinetic parameters of similar systems.[43c,50] This mechanism would exhibit unchanged kinetics of the reorganization of **2** to **1** in the presence of external CO, but the occurrence of up to 25% label incorporation in the product in the presence of external ^{13}CO. Surprisingly, monitoring of the disappearance of **2** under atmospheric CO (85 °C) revealed a rate *increase* [k(N2) = 2.51 × 10^{-2} min^{-1} vs k(CO) = 1.35 × 10^{-1} min^{-1} in diglyme], accentuated by increasing the external CO pressure, signalling (again) a change in mechanism. Following the process with added ^{13}CO by ^{13}C NMR spectroscopy (THF-d_8) established uptake of labeled ligand in the product (40% by mass spectrometry), but not in unreacted starting material. A control experiment showed that **1** was inert under these conditions. Thus, external CO was added or was incorporated during the irreversible formation of some intermediate in the transformation of **2** to **1**.

A plausible pathway that is consistent with the above results involves attack by the external ligand on a Ru atom in **2** to cause C−C bond coupling, providing an intermediate zwitterion **24a** which subsequently forms a metal−metal bond and ejects CO (Scheme 6). Zwitterionic Fv complexes analogous to **24a** have been isolated and structurally characterized,[6a,b,d,f] but they are all stabilized by phosphine ligands on the cationic metal fragment and their conversion to metal−metal-bonded species is only possible via ligand extrusion promoted by photolysis or reduction−oxidation sequences.[6a,b] In **24a**, the tricarbonyl cation moiety would be expected to be relatively reactive with respect to ligand loss, and metal−metal bond formation would thus be facile. In addition, multiple label exchange might occur rapidly, thus explaining the observation of the higher than expected 40% ^{13}CO incorporation.

Support for the plausibility of ligand-induced coupling of the Cp rings in **2** was obtained in studies of its reactivity with other potential ligands. Thus, qualitatively, the rearrangement of **2** to **1** is greatly accelerated in CH_3CN solvent, being complete within minutes at 23 °C. More quantitatively, when a solution of **2** in THF-d_8 was treated with an excess of $P(CH_3)_3$ (∼8 equiv) at room temperature, the ring slippage (metal decomplexation) products **25** and **26** in addition to **27** were formed within 2 h in quantitative yield (^{1}H NMR) in the indicated ratio (Scheme 6). At 0 °C, the reaction was more sluggish (97% complete in 3 days) and the ratio of **25** to **26** was greater (10.5:2). This finding suggested that the initial product **25** subsequently transformed into **26**. Indeed, when the former was heated (80 °C) or

(43) (a) For an "unusually low" value of a Ru−CH_2CH_3 bond (21.7 kcal mol^{-1}), see: Collman, J. P.; McElwee-White, L.; Brothers, P. J.; Rose, E. *J. Am. Chem. Soc.* **1986**, *108*, 1332. (b) Bryndza, H. E.; Fong, L. K.; Paciello, R. A.; Tan, W.; Bercaw, J. E. *J. Am. Chem. Soc.* **1987**, *109*, 1444. (c) Bryndza, H. E.; Domaille, P. J.; Paciello, R. A.; Bercaw, J. E. *Organometallics* **1989**, *8*, 379. (d) Martinho Simões, J. A.; Beauchamp, J. L. *Chem. Rev.* **1990**, *90*, 629. (e) Mancuso, C.; Halpern, J. *J. Organomet. Chem.* **1992**, *428*, C8. (f) A bond energy of 40 kcal mol^{-1} for Cp*Ru-$[P(CH_3)_3]_2$−Ph is given: Drago, R. S.; Wong, N. M.; Ferris, D. C. *J. Am. Chem. Soc.* **1992**, *114*, 91. (g) Luo, L.; Li, C.; Cucullu, M. E.; Nolan, S. P. *Organometallics* **1995**, *14*, 1333.

(44) Qualitatively, the $\mathrm{CpRuL_2}\sigma$-cyclopentadienyl (ferrocenyl) bond appears to be thermally quite robust: (a) Herberhold, M.; Feger, W. *J. Organomet. Chem.* **1992**, *436*, 333. (b) Lehmkuhl, H. *Pure Appl. Chem.* **1990**, *62*, 731. (c) Lehmkuhl, H.; Schwickardi, R.; Krüger, C.; Raabe, G. *Z. Anorg. Allg. Chem.* **1990**, *581*, 41. (d) See also ref 19c,d.

(45) See, inter alia: (a) Pugh, J. R.; Meyer, T. J. *J. Am. Chem. Soc.* **1992**, *114*, 3784. (b) Corraine, M. S.; Atwood, J. D. *Organometallics* **1991**, *10*, 2315. (c) Pilcher, G.; Skinner, H. A. In *The Chemistry of the Metal Carbon Bond*; Hartley, F. R., Patai, S., Eds.; Wiley: New York, 1982; Chapter 2. (d) Kovács, I.; Baird, M. C. *Organometallics* **1995**, *14*, 5469.

(46) In the consideration of biradical vs concerted pathways, it is instructive to compare the $\Delta S^{\ddagger}$ values in the extensively investigated hydrocarbon rearrangements: Gajewski, J. J. *Hydrocarbon Thermal Isomerizations*; Academic Press: New York, 1981.

(47) Chlorinated solvents react with organometallic compounds by a variety of mechanisms. For very recent work, see, inter alia: (a) McElwee-White, L. *Synlett* **1996**, 806. (b) Jernakoff, P.; Fox, J. R.; Cooper, N. J. *J. Organomet. Chem.* **1996**, *512*, 175. (c) Dos Santos, J. E.; Peppe, C.; Brown, M. A.; Tuck, D. G. *Organometallics* **1996**, *15*, 2201.

(48) For a recent monograph, see: Astruc, D. *Elecron Transfer and Radical Processes in Transition-Metal Chemistry*; VCH: Weinheim, 1995.

(49) For reviews, see: (a) Basolo, F. *Polyhedron* **1990**, *9*, 1503. (b) Poe, A. J. In *Mechanisms of Inorganic and Organometallic Reactions*; Twigg, M. V., Ed.; Plenum: New York, 1994.

(50) (a) Brown, D. A.; Lyons, H. J.; Sane, R. T. *Inorg. Chim. Acta* **1970**, *4*, 621. (b) Huq, R.; Poe, A. J.; Chawla, S. *Inorg. Chim. Acta* **1980**, *38*, 12 1. (c) Atwood, J. D. *J. Organomet. Chem.* **1990**, *383*, 59. (d) Luginbühl, W.; Zbinden, P.; Pittet, P. A.; Armbruster, T.; Bürgi, H.-B.; Merbach, A. E.; Ludi, A. *Inorg. Chem.* **1991**, *30*, 2350.

Scheme 6

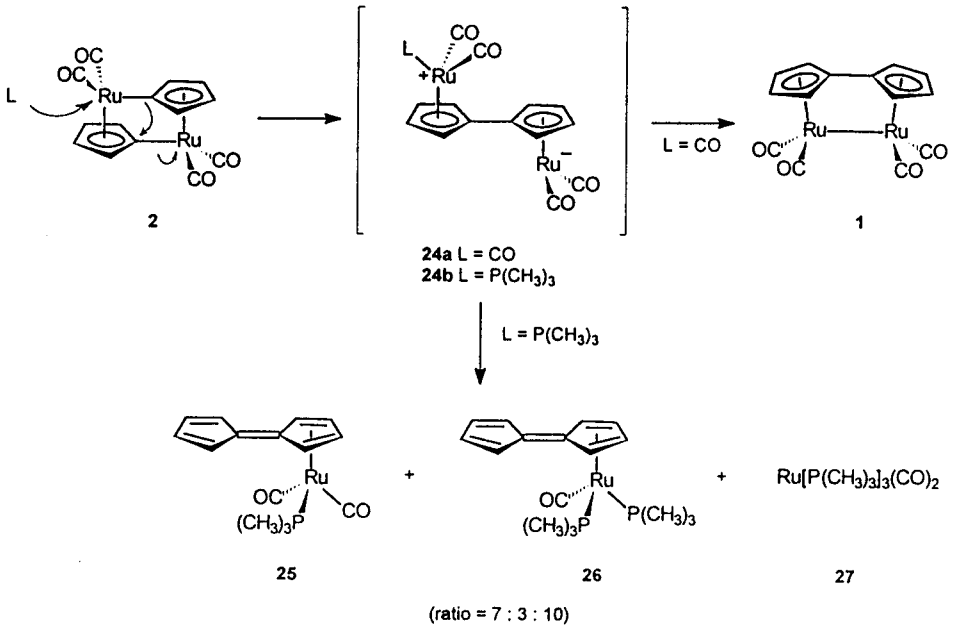

irradiated (350 nm) in the presence of $P(CH_3)_3$, it cleanly underwent carbonyl substitution to **27**. No intermediates or other species in the reaction of **2** with $P(CH_3)_3$ were detected at 0 °C or at room temperature by ^1H or $^{31}P\{^1H\}$ NMR spectroscopy. Qualitative experiments established a clear rate acceleration when the concentration of the phosphine reagent was increased. Interestingly, **26** and **27** (1:1) arise also when **1** is treated with excess $P(CH_3)_3$, but in this instance more drastic conditions are necessary to effect ring slippage (120 °C, 22 h).[7d] It appears that the relative thermodynamic stabilities of **1** and **2** are reflected in their relative reactivities.

Complexes **26** and **27** were identified by comparison of their ^1H and $^{31}P\{^1H\}$ NMR spectra with data either reported in the literature (**26**)[7d] or, for **27**, obtained from a sample prepared independently via treatment of **13** with $P(CH_3)_3$ at 120 °C for 24 h. Although not isolated because of difficulties encountered in attempts to separate it from **26**, **25** was identified on the basis of the similarity of its ^1H and $^{31}P\{^1H\}$ NMR spectra to those of **26** and the presence of two bands in the carbonyl region of its IR spectrum (2017 and 1961 cm^{-1} in THF). The peaks due to the Fv hydrogens in its ^1H NMR spectrum are shifted downfield from those of **26**, consistent with a more electron-poor system as expected on the basis of the presence of only a single phosphine ligand. Furthermore, the presence of only one $P(CH_3)_3$ group was confirmed by the appearance of a singlet in the $^{31}P\{^1H\}$ NMR and a doublet ($J = 10.5$ Hz) at 1.27 ppm in the ^1H NMR spectrum.

Because of the complications encountered when executing the **2** → **1** isomerization in the presence of external ^{13}CO, a crossover labeling study was performed. In this experiment, a 1:1 mixture of **2** and **2**-(60% ^{13}CO) was transformed into **1** and **1**-(^{13}CO) in hot DME and analyzed by mass spectroscopy. Computer simulation[51] of the statistical distribution of label expected for various degrees of exchange and comparison with the experimental spectra revealed the *absence of any intermolecular CO scrambling*. Thus, CO dissociation prior to (or during) rearrangement is not a mechanistic pathway traversed in the thermal isomerization of **2**.

Summary and Conclusions

The photochemical isomerization of **1** to **2** and its thermal reverse constitute a light energy storage−thermal release cycle that is clean, relatively efficient, and energy rich. It also poses a mechanistic challenge. The conditions under which it occurs cleanly appear to require specifically the $FvRu_2$ frame, bearing relatively π-acidic ligands [CO, $P(OCH_3)_3$], the use of relatively low-energy radiation (350 nm to sunlight), and the absence of external species that are capable of attacking **2** directly.

For both halves of the cycle, CO dissociation, dissociative cleavage to two $(C_5H_4)Ru(CO)_2$ halves, single inversion, and a switch in Cp−Ru connectivity have been ruled out. Dipolar intermediates appear unlikely on the basis of quantum yield and kinetic data, respectively. Biradical species cannot be excluded from consideration, but are not directly indicated in either process and, if involved, would require ad hoc justification. As an operational suggestion, in the absence of evidence to the contrary and supporting alternatives[52] and ignoring the difference in the electronic details of the two manifolds (excited versus ground state) but focusing purely on topology, we conclude that **1** and **2** transform into each other in a concerted manner (Scheme 2). Further probing of the scope and limitations and the mechanisms by which modified versions of **1** and **2** transform will be the subject of future investigations.

Experimental Section

General Procedures. Unless otherwise indicated, all manipulations were conducted under purified N_2 either in a Vacuum Atmospheres Inc. glovebox or using standard Schlenk vacuum line techniques. Tetrahydrofuran (THF), dimethoxyethane (DME), and diethyl ether (Et_2O) were distilled from either potassium or sodium benzophenone ketyl immediately prior to use. Diethylene glycol dimethyl ether (diglyme), decane, and acetonitrile were distilled from sodium, lithium aluminum hydride, or calcium hydride, respectively. Chromatography solvents were deoxygenated by purging with a stream of N_2. $FvRu_2(CO)_4$ (**1**),[7b] *tert*-butylcyclopentadiene,[53] and $NaCp(DME)$[54] were

(51) This problem is intractable by simple analysis, because (1) Ru has seven natural isotopes, generating 16 readily observable peaks in the mass spectra of **1** and **2**, (2) ^{13}CO enrichment of **2**-(^{13}CO) was not complete, (3) the commercial ^{13}CO used (Cambridge Isotope Laboratories, Inc.) contains approximately 10% ^{18}O, and (4) natural abundance ^{13}C in the samples had to be considered. We thank Mr. D. Peterson and Professor J. Rice, UCB Department of Statistics for their help in solving it.

(52) Hoffmann, R.; Minkin, V. I.; Carpenter, B. K. *Bull. Soc. Chim. Fr.* **1996**, *133*, 117.

(53) Riemschneider, R.; Nehring, R. *Monatsh. Chem.* **1959**, *90*, 568.

(54) Smart, J. C.; Curtis, C. J. *Inorg. Chem.* **1978**, *17*, 3290.

prepared by literature methods. Crystals of **1** suitable for analysis by X-ray diffraction were obtained by slow diffusion of pentane into a saturated acetone solution at 0 °C. All other chemicals were obtained from commercial suppliers and used without further purification.

Photoreactions were performed either in Pyrex vessels employing a GE ELH 300 W projector or near-UV lamps of primary output between 325 and 375 nm (λ_{max} at 350 mn) or in quartz tubes with UV lamps having $\lambda_{max} = 300$ nm. High-pressure liquid chromatography (HPLC) utilized an Altex Model 110A liquid chromatograph (silica 60 column) connected to a Hitachi Model 100−10 variable wavelength detector.

^{1}H NMR spectra were recorded on UC Berkeley (UCB) 200, 250, or 300 MHz instruments equipped with Cryomagnets, Inc., superconducting magnets and Nicolet Model 1180 or 1280 data collection systems. ^{13}C{^{1}H} and ^{31}P{^{1}H} NMR spectra were measured at 75 and 121.5 MHz, respectively, on the UCB 300 instrument. ^{1}H and ^{13}C{^{1}H} NMR spectra are reported in ppm downfield from tetramethylsilane and are referenced to the resonances of the deuterated solvent. ^{31}P{^{1}H} NMR chemical shifts are quoted relative to 85% H_3PO_4. ^{1}H−^{1}H COSY and NOE difference spectra were acquired on the UCB-300 or on a Bruker AM-500 instrument. Line shape analyses of variable temperature spectra were carried out as outlined in ref 30. IR spectra were measured on a Perkin-Elmer Model 681 spectrophotometer and UV−vis absorptions on a Hewlett-Packard Model 8450A UV−vis Diode Array system. Mass spectral data were provided by the UCB Mass Spectrometry Laboratory and collected on either an AEI-MS12 mass spectrometer at 70 eV or a Finnigan 4000 instrument. Chemical ionization (CI) techniques used methane, whereas fast atom bombardment (FAB) studies relied on glycerol, nitrobenzyl alcohol (NBA), or tetramethylene sulfone (TMES) matrices. Because the natural isotopic distribution of Ru resulted in broad peak envelopes, only the major peak for each fragment is reported. Elemental analyses were carried out by the UCB Microanalytical Laboratory. Melting points were observed in sealed glass capillaries under N_2 on a Büchi melting point apparatus and are uncorrected.

(μ_2-η^1:η^5-Cyclopentadienyl)$_2$Ru$_2$(CO)$_4$ (2). A solution of **1** (0.884 g, 2.0 mmol) in THF (400 mL) was placed in five 12 in. × 1 in. Pyrex tubes and irradiated with 350 nm light for 2 h. The contents of the vessels were combined, diluted with heptane (50 mL), concentrated to saturation by vacuum transfer without heating, and chromatographed on alumina(II) using pentane as eluent. Slow removal of solvent under reduced pressure and at ambient temperature yielded crystalline **2** (0.548 g, 62%). Subsequent elution with CH_2Cl_2 allowed recovery of a yellow band containing unreacted **1** (0.195 g, 22%). Crystals of **2** suitable for analysis by X-ray diffraction were grown by diffusion of pentane into a saturated THF solution at −20 °C. For complex **2**: colorless crystals, isomerization point 208 °C; ^{1}H NMR (200 MHz, $CDCl_3$) δ 4.68 (dd, $J = 2.1$, 2.1 Hz, 4H), 5.39 (dd, $J = 2.1$, 2.1 Hz, 4H); ^{13}C{^{1}H} NMR (THF-d_8) δ 85.8, 91.7, 96.8, 202.1; IR (KBr) ν_{CO} 2000, 1960 cm^{-1}; UV (THF) λ_{max} 239 (ϵ 7900), 286 (1500) nm; MS *m/z* (rel intensity) 443 (M$^+$, 81), 359 (M$^+$ − 3CO, 100), 331 (M$^+$ − 4CO, 32). Anal. Calcd for $C_{14}H_8O_4Ru_2$: C, 38.03; H, 1.82. Found: C, 38.27; H, 2.01.

Determination of the Enthalpy of the Isomerization of 2 to 1. Samples of **2** were weighed (±0.001 mg) and sealed under He into aluminum sample dishes at the UCB Microanalytical Laboratory. Analyses by differential scanning calorimetry (DSC) were conducted on a Perkin-Elmer Model PE-2 DSC. The instrument was calibrated before, during, and after each analysis against a similarly prepared indium standard (indium mp = 156 °C, $\Delta H_{fusion} = 6.82$ kcal mol^{-1}), revealing an enthalpy change of −29.8 (1.5) kcal mol^{-1} for the isomerization of **2** to **1**.

(η^5:η^5-Fulvalene)(μ_2-η^1:η^5-cyclopentadienyl)$_2$Ru$_4$(CO)$_6$ (6). A solution of **2** (0.177 g, 0.40 mmol) in THF (80 mL) in a quartz tube was irradiated with 300 nm light under a constant N_2 purge for **1** h. Concentration to ∼10 mL and chromatography on alumina(II) with Et_2O as eluant gave **2** and a minor amount of **1** (<10 mg), followed closely by a broad purple band containing **6** (68 mg, 41%). Purple-black tabular crystals suitable for analysis by X-ray diffraction were prepared by diffusion of pentane into a CH_2Cl_2 solution: mp 260 °C (dec.); ^{1}H NMR (200 MHz, acetone-d_6) δ 3.45 (m, 1H), 3.68 (m, 1H), 4.08 (m, 1H), 4.28 (m, 1H), 4.60 (m, 1H), 4.70 (m, 1H), 4.91 (m, 1H), 4.95 (m, 1H), 4.99 (m, 1H), 5.12 (m, 1H), 5.25 (m, 1H), 5.40 (m, 1H), 5.52 (m, 1H), 5.66 (m, 1H), 5.73 (m, 1H), 5.94 (m, 1H); IR (KBr) ν_{CO} 2002, 1956, 1944, 1938, 1900, 1775, 1762 cm^{-1}; CI-MS *m/z* (rel intensity) 829 (M$^+$, 7), 803 (M$^+$ − CO, 1), 774 (M$^+$ − 4CO, 8), 444 [FvRu$_2$(CO)$_4$, 64], 417 [FvRu$_2$(CO)$_2$, 81]. Anal. Calcd for $C_{26}H_{16}O_6Ru_4$: C, 37.69; H, 1.95. Found: C, 37.87; H, 1.95.

(η^5:η^5-Fulvalene)(μ_2-η^2-ethyne)Ru$_2$(CO)$_3$ (8). A solution of **1** or **2** (88.4 mg, 0.20 mmol) in THF (80 mL) sealed in a quartz tube and saturated with ethyne was irradiated with 300 nm light for 2 h. To the resulting orange-brown liquid was added alumina(II) (20 g), and the solvent was removed under vacuum. Chromatography of the adsorbed sample (alumina(II), 1:1 pentane−Et_2O) afforded **8** [orange band, eluted after small amounts (<5 mg) of **2** and **1**], isolated as orange crystals by slow evaporation of solvent (49 mg, 56%) or, for X-ray crystallography, from acetone−pentane under an atmosphere of ethyne: mp 205 °C (dec.); ^{1}H NMR (200 MHz, acetone-d_6) δ 4.80 (m, 2H), 5.15 (m, 2H), 5.72 (m, 2H), 6.03 (m, 2H), 6.86 (s, 2H); IR (KBr) ν_{CO} 1980, 1944, 1755 cm^{-1}; CI-MS *m/z* (rel intensity) 442 (M$^+$, 78), 414 (100). Anal. Calcd for $C_{15}H_{10}O_3Ru_2$: C, 40.91; H, 2.28. Found: C, 41.11; H, 2.03.

(η^5:η^5-Fulvalene)(μ_2-η^2-diphenylethyne)Ru$_2$(CO)$_3$ (9). A solution of **1** (88.4 mg, 0.20 mmol) and diphenylethyne (71.2 mg, 0.40 mmol) in THF (80 mL) in a quartz tube was irradiated with 300 nm light for 4 h, while being purged with N_2. Adsorption onto alumina(II) and chromatography as in the preparation of **8** yielded **9** (75 mg, 63%): red crystals (from 1:1 pentane−Et_2O), mp 220 °C (dec.); ^{1}H NMR (200 MHz, acetone-d_6) δ 4.84 (m, 2H), 5.58 (m, 2H), 5.64 (m, 2H), 6.16 (m, 2H), 6.97 (m, 10H); IR (KBr) ν_{CO} 1992, 1970, 1770 cm^{-1}. Anal. Calcd for $C_{27}H_{18}O_3Ru_2$: C, 54.73; H, 3.06. Found: C, 54.45; H, 3.11.

(η^5:η^5-Fulvalene)(μ_2-η^2-dimethyl butynedioate)Ru$_2$(CO)$_3$ (10). A solution of **1** (88.4 mg, 0.20 mmol) and dimethyl butynedioate (66.4 mg, 0.40 mmol) in THF (80 mL) was irradiated, and the resulting mixture adsorbed onto alumina, as in the preparation of **9**. Chromatography with Et_2O as eluent (alumina(II)) afforded a small amount of **2** and unreacted **1** (<5 mg). Subsequent elution with acetone−Et_2O (1:4) gave **10**, isolated as yellow-orange crystals by slow evaporation of solvent (88 mg, 76%): mp 200 °C (dec.); ^{1}H NMR (200 MHz, acetone-d_6) δ 3.55 (s, 6H) 4.89 (m, 2H), 5.36 (m, 2H), 5.74 (m, 2H), 6.21 (m, 2H); IR (KBr) ν_{CO} 1980, 1775, 1690 cm^{-1}. Anal. Calcd for $C_{19}H_{14}O_7Ru_2$: C, 41.01; H, 2.54. Found: C, 41.19; H, 2.67.

Comparison of the Photoreactivities of 1 and 2. Solutions (10 mL, 0.001 M) of **1** and **2** in 1.0 cm OD quartz tubes held in a rotating sample holder were irradiated simultaneously with 300 nm light for the time periods indicated in Table 2. Without delay, the solvent was removed by an N_2 stream and the composition of the residue was analyzed by ^{1}H NMR spectroscopy (acetone-d_6).

(η^5:η^5-Fulvalene)Ru$_2$(CO)$_3$ [P(CH$_2$CH$_3$)$_3$] (12). To a solution of **1** (0.10 g, 0.23 mmol) in THF (8 mL) in a Pyrex bomb fitted with a Teflon stopcock was added P(CH$_2$CH$_3$)$_3$ (300 μL, 2.0 mmol). The mixture was degassed, heated to 120 °C for 20 h, and cooled, and the volatiles were removed under vacuum. The resulting orange residue was filtered through activated alumina eluting with THF. Subsequent addition of hexanes and cooling (0 °C) afforded crystalline **12** (70 mg, 58%): orange blades, mp 226−228 °C; ^{1}H NMR (300 MHz, acetone-d_6) δ 1.02 (dt, $J = 15.6$, 7.7 Hz, 9H), 1.80 (dq, $J = 8.4$, 7.7 Hz, 6H), 4.20 (dd, $J = 2.1$, 2.1 Hz, 2H), 4.22 (dd, $J = 2.2$, 2.2 Hz, 2H), 5.29 (dd, $J = 2.1$, 2.1 Hz, 2H), 5.69 (dd, $J = 2.2$, 2.2 Hz, 2H); ^{13}C{^{1}H} NMR (THF-d_8, 20 °C) δ 9.0, 25.2 (d, $J = 28.4$ Hz), 75.6 (br s), 79.6, 83.9 (br s), 88.0, 92.5, 93.0, 207.9, 210.5 (d, $J = 9.8$ Hz); ^{31}P{^{1}H} NMR (acetone-d_6) δ 46.51 (s); IR (THF) ν_{CO} 1983, 1917, 1887 (w) cm^{-1}; UV (THF) λ_{max} 275 (ϵ 11 200), 338 (6300), 460 (1200) nm; MS *m/z* (rel intensity) 553 (M$^+$, 9), 69 (100). Anal. Calcd for $C_{19}H_{23}O_3PRu_2$: C, 42.86; H, 4.35. Found: C, 43.04; H, 4.42.

(η^5:η^5-Fulvalene)Ru$_2$(CO)$_3$[P(CH$_3$)$_3$] (13). A solution of **1** (0.10 g, 0.23 mmol) in THF (8 mL) was exposed to P(CH$_3$)$_3$ (60 μL, 0.70 mmol) at 150 °C for 36 h, as in the preparation of **12**. Two crystallizations of the resulting orange oil from THF−hexanes gave **13** (52 mg, 44%): orange prisms, mp 162−163 °C; ^{1}H NMR (300 MHz, acetone-d_6) δ 1.53 (d, $J = 9.5$ Hz, 9H), 4.10 (dd, $J = 2.2$, 2.2 Hz, 2H), 4.19 (dd, $J = 2.1$, 2.1 Hz, 2H), 5.31 (dd, $J = 2.1$, 2.1 Hz, 2H), 5.68 (dd, $J = 2.2$, 2.2 Hz, 2H); ^{13}C{^{1}H} NMR (acetone-d_6, 20 °C) δ 24.3 (d, $J = 31.2$ Hz), 76.5 (br s), 80.0, 84.5 (br s), 88.3, 93.0, 93.5; ^{31}P{^{1}H} NMR (acetone-d_6) δ 12.65 (s); IR (THF) ν_{CO} 1980, 1917, 1900 (sh) cm^{-1}; UV (THF) λ_{max} 257 (ϵ 15 800), 333 (8700), 444 (1260)

nm; CI-MS *m/z* (rel intensity) 491 ($M^+ - CO$, 100). Anal. Calcd for $C_{16}H_{17}O_3PRu_2$: C, 39.19; H, 3.49. Found: C, 39.52; H, 3.49.

(η^5:η^5-Fulvalene)$Ru_2(CO)_3[P(OCH_3)_3]$ (14). A solution of **1** (300 mg, 0.70 mmol) in THF (10 mL) was exposed to $P(OCH_3)_3$ (300 μL, 2.5 mmol) at 120 °C for 22 h, as in the preparation of **12** and **13**. Chromatography of the crude product on activated alumina with toluene−hexanes (2:3) as eluant resulted first in recovered **1** (<10 mg), followed by a deep yellow fraction. After solvent evaporation, crystallization from THF−hexanes afforded **14** (236 mg, 65%): bright yellow powder, mp 155−157 °C; ^{1}H NMR (300 MHz, acetone-d_6, 25 °C) δ 3.47 (d, J = 12.2 Hz, 9H), 4.23 (br s, 4H), 5.47 (br s, 2H), 5.72 (dd, J = 2.0, 2.0 Hz, 2H); ^{13}C{^{1}H} NMR (acetone-d_6, 25 °C) δ 52.1 (d, J = 2.8 Hz), 77.0 (br s), 79.6, 84.5 (br s), 86.0 (br s), 87.5 (br s), 93.3, 93.4, 208.1, 208.7; ^{31}P{^{1}H} NMR (acetone-d_6) δ 172.7 (s); IR (THF) ν_{CO} 1988, 1932, 1915 (sh) cm^{-1}; UV (THF) λ_{max} 272 (ϵ 12 600), 333 (7400), 418 (1100) nm; MS *m/z* (rel intensity) 539 (M^+, 34), 331 [$M^+ - 3CO$, $P(OCH_3)_3$, 100]. Anal. Calcd for $C_{16}H_{17}O_6PRu_2$: C, 35.69; H, 3.18. Found: C, 35.52; H, 3.26.

(μ_2-η^1:η^5-Cyclopentadienyl)$_2$[$Ru(CO)_2$][$Ru(CO)${$P(OCH_3)_3$}] (15). A solution of **14** (50 mg, 0.09 mmol) in THF (50 mL) was irradiated with a tungsten light projector lamp for 2.5 h. Solvent was removed, and the residue was chromatographed on activated alumina eluting with Et_2O−hexanes (3:7) to give a colorless fraction. Crystallization from hexanes afforded **15** (33 mg, 66%): colorless crystals, mp 82−83 °C; ^{1}H NMR (300 MHz, acetone-d_6) δ 3.50 (d, J = 12.2 Hz, 9H), 4.29 (dddd, J = 2.2, 1.6, 1.6, 1.5 Hz, 1H), 4.66 (dddd, J = 4.9, 2.1, 1.5, 1.4 Hz, 1H), 4.77 (dd, J = 3.8, 1.7 Hz, 1H), 4.81 (dd, J = 3.8, 1.7 Hz, 1H), 5.14 (m, 1H), 5.21 (m, 1H), 5.44 (ddd, J = 3.8, 2.0, 1.7 Hz, 2H); ^{31}P{^{1}H} NMR (THF-d_8) δ 168.4 (s); IR (THF) ν_{CO} 2015, 1963, 1947 cm^{-1}; UV (THF) λ_{max} 241 (ϵ 5900), 282 (2500) nm; FAB-MS (TMES) *m/z* 540 ($M^+ + 1$), 511 ($M^+ - CO$), 483 ($M^+ - 2CO$), 453 ($M^+ - 3CO$). Anal. Calcd for $C_{16}H_{17}O_6PRu_2$: C, 35.69; H, 3.18. Found: C, 35.82; H, 3.19.

Crossover Experiment. An equimolar mixture of **1** (88.4 mg, 0.20 mmol) and **1**-d_8 (90.0 mg) was dissolved in diglyme (200 mL) and a sample submitted for three replicate mass spectral analyses. The bulk of the solution was irradiated using 350 mn light for 2 h, at which time ^{1}H NMR analysis of an aliquot revealed >80% isomerization to **2**. The liquid was then heated to reflux for 2 h, resulting in the complete conversion of **2** back to **1**. This cycle was then repeated twice, after which the sample was submitted for three replicate mass spectrometric analyses. A comparison of peak intensities for a range of test peaks only significant in the spectrum of **1** (*m/z* 434−440) and a range only significant in the spectrum of **1**-d_8 (*m/z* 446−452) with the intensity of the peak at *m/z* 445, predicted by computer simulation to experience the greatest enhancement upon formation of the hypothetical d_4-crossover product, revealed the absence of significant differences between the samples analyzed before and after the three isomerization cycles, indicating that crossover had not occurred.

Quantum Yield Measurements. Approximate quantum yields for the photoisomerization of **1** to **2** and, for comparison, the photooxidation of $Cp_2Ru_2(CO)_4$ by CCl_4 to $CpRu(CO)_2Cl$ were determined using the standard method of potassium ferrioxalate actinometry. Both actinometer standards and samples (sealed under N_2) were irradiated in 1.0 cm Pyrex tubes held in a rotating carousel holder and suspended in a Rayonet reactor. Irradiations were performed with the reactor half filled with RPR-3500A lamps (λ_{max} = 350 nm) at room temperature. Data were collected for irradiation intervals resulting in less than 10% actinometer depletion and less than 15% sample conversion to products. Yields for the photoisomerization of **1** to **2** were measured in pure acetone-d_6, CD_2Cl_2, and THF-d_8, in 1.0 M solutions of CCl_4 in these same solvents, and in CO-saturated THF-d_8. The initial concentration in all cases was 2.2×10^{-3} M. After exposure, each sample was transferred directly via syringe into an NMR tube and the conversion to product assessed by integration. The absence of significant decomposition was verified by a comparison of the integration ratios after photolysis to those before, relative to the residual solvent peak. Each entry in Table 4 represents an average quantum yield from three experiments.

(*S,*S**- and *S**,*R**-3,3′-Di-*tert*-butylfulvalene)$Ru_2(CO)_4$ (19a and 19b).** Butyllithium (31.0 mL, 1.6 M in hexane) was added to a stirred solution of *tert*-butylcyclopentadiene (5.92 g, 0.049 mol) in THF (90 mL) at −78 °C. The mixture was allowed to warm slowly (2 h) to RT and was then cooled again to −78 °C. Subsequently, iodine (6.35 g, 0.025 mol) in THF (15 mL) was injected with a syringe, the temperature was allowed to warm toward RT for 25 min, and heptane (100 mL) was added, followed after 2 min by quenching the reaction with a 1% aqueous $Na_2S_2O_3$ solution (100 mL). After an additional minute of stirring, the mixture was poured into an N_2-flushed separatory funnel, the aqueous layer was discarded, and the orange organic fraction was dried over Na_2SO_4 for 5 min, decanted under N_2, cooled to −78 °C, and added via syringe over 23 h to a boiling solution of $Ru_3(CO)_{12}$ (7.03 g, 0.011 mol) in DME (400 mL). After it had been heated to reflux for 18 h, the mixture was cooled, passed through an activity III alumina column (250 g, CH_2Cl_2), and the resulting orange solid chromatographed on activated alumina. A yellow fraction was collected on elution with toluene−hexanes (1:9), the contents of which precipitated from CH_2Cl_2−hexanes (0 °C) to give a mixture of **19a** and **19b** (3.16 g, 35%). The isomers were separated by HPLC [toluene−hexanes (1:10), flow rate 4.2 mL min^{-1}, monitoring wavelength 330 nm] to give first **19a** and then **19b** as yellow powders. For **19a** and **19b**: IR (CH_2Cl_2) ν_{CO} 2016, 1948 cm^{-1}; UV (THF) λ_{max} 243 (ϵ 14 500), 272 (12 000), 330 (8100), 400 (sh, 1600) nm; MS *m/z* (rel intensity) 555 (M^+, 50), 434 ($M^+ - 4CO$, 100). Anal. Calcd for $C_{22}H_{24}O_4Ru_2$: C, 47.65; H, 4.36. Found: C, 47.67; H, 4.45. For **19a**: mp 208−210 °C (dec.); ^{1}H NMR (250 MHz, $CDCl_3$) δ 1.25 (s, 18H), 3.74 (dd, J = 2.0, 2.7 Hz, 2H), 3.85 (dd, J = 1.9, 1.9 Hz, 2H), 5.58 (dd, J = 1.9, 2.8 Hz, 2H); ^{13}C{^{1}H} NMR ($CDCl_3$) δ 30.8, 31.9, 75.4, 76.2, 85.2, 91.4, 126.6, 205.6, 206.2. For **19b**: mp 185−186 °C (dec.); ^{1}H NMR (250 MHz, $CDCl_3$) δ 1.26 (s, 18H), 3.74 (dd, J = 2.6, 2.1 Hz, 2H), 3.85 (dd, J = 1.8, 1.8 Hz, 2H), 5.57 (dd, J = 2.6, 2.0 Hz, 2H); ^{13}C{^{1}H} NMR ($CDCl_3$) δ 30.8, 31.9, 75.3, 76.2, 85.2, 91.4, 126.7, 205.3, 206.4.

(*S-μ_2-η^1:η^5-3-*tert*-Butylcyclopentadienyl)(*S**-μ_2-η^1:η^5-3′-*tert*-butylcyclopentadienyl)$Ru_2(CO)_4$ (20a) and (*S**-μ_2-η^1:η^5-3-*tert*-butylcyclopentadienyl)(*R**-μ_2-η^1:η^5-3′-*tert*-butylcyclopentadienyl)$Ru_2(CO)_4$ (20b).** A solution of a mixture of **19a** and **19b** (1:1, 50 mg, 0.09 mmol) in THF (60 mL) in a Pyrex test tube was irradiated with 350 nm light for 4 h. Chromatography on activity II alumina with hexanes as eluent gave a mixture of photoisomers **20a** and **20b** (1:1, 33 mg, 67%). Similar treatment of pure **19a** afforded **20a**, while **19b** gave **20b**. Each isomer could be crystallized by slow cooling of a a saturated hexanes solution. For **20a** and **20b**: IR (CH_2Cl_2) ν_{CO} 2007, 1953 cm^{-1}; UV (THF) λ_{max} 233 (ϵ 7900), 302 (1600) nm; FAB-MS (NBA) *m/z* 556 ($M^+ + 1$). Anal. Calcd for $C_{22}H_{24}O_4Ru_2$: C, 47.65; H, 4.36. Found: C, 47.84; H, 4.35. For **20a**: colorless crystals, mp 114−115 °C; ^{1}H NMR (300 MHz, THF-d_8) δ 1.19 (s, 18H), 4.62 (dd, J = 2.1, 2.0 Hz, 2H), 4.86 (dd, J = 1.8, 1.8 Hz, 2H), 5.51 (dd, J = 2.1, 2.0 Hz, 2H); ^{13}C{^{1}H} NMR (C_6D_6) δ 30.4, 32.0, 85.2, 87.7, 93.7, 94.6, 130.3, 202.0, 202.5. For **20b**: colorless crystals, mp 158−160 °C; ^{1}H NMR (300 MHz, THF-d_8) δ 1.18 (s, 18H), 4.65 (dd, J = 2.2, 2.0 Hz, 2H), 4.83 (dd, J = 1.8, 1.8 Hz, 2H), 5.53 (dd, J = 2.2, 2.0 Hz, 2H); ^{13}C{^{1}H} NMR (C_6D_6) δ 30.4, 32.0, 85.2, 87.7, 93.8, 94.5, 130.4, 201.8, 202.7.

(3-*tert*-Butylfulvalene)$Ru_2(CO)_4$ (21). Methyllithium (8.93 mL, 1.4 M in Et_2O) was added dropwise over 10 min to a solution of 6,6-dimethylfulvene (1.32 g, 12.5 mmol) in Et_2O (15 mL) at 0 °C. After the mixture was stirred at 0 °C for an additional 45 min, THF (30 mL) was added. The resulting clear, colorless solution was cooled to −78 °C and slowly added via cannula to iodine (3.30 g, 13 mmol) in cold (−78 °C) THF (20 mL). The iodine solution decolorized and turned into an orange slurry. After an additional 5 min of stirring at −78 °C, a solution of NaCp(DME) (2.32 g, 13 mmol) in THF (30 mL) was added via cannula. The resulting orange mixture was allowed to wann toward RT for 20 min and was then treated with aqueous $Na_2S_2O_3$−heptane (1:1, 200 mL) in the usual manner (see preparation of **19a** and **19b**). The heptane fraction was cooled to −78 °C and added to $Ru_3(CO)_{12}$ (2.13 g, 3.3 mmol) in boiling DME (300 mL) over 2−3 h. After having been heated to reflux overnight, the orange solution was cooled and the solvent was removed by rotary evaporation. Chromatography on activated alumina eluting with toluene−hexanes (3:7) gave a small amount of **19a** and **19b** (∼50 mg) followed by **21** (734 mg, 29%): yellow powder, mp 184−185 °C; ^{1}H NMR (300 MHz, THF-d_8) δ 1.28 (s, 9H), 4.10 (dd, J = 2.7, 2.0 Hz, 1H), 4.20 (ddd, J = 2.2, 2.0, 1.9 Hz, 1H), 4.23 (ddd, J = 2.2, 2.1, 1.9 Hz, 1H), 4.27 (dd, J = 1.8, 1.8 Hz, 1H), 5.79 (dd, J = 2.2, 2.0 Hz, 2H); ^{13}C{^{1}H} NMR (THF-d_8) δ 31.6, 32.2, 77.0, 77.8, 79.1, 79.2, 86.4, 88.9, 92.2, 95.1, 127.7,

206.1, 206.2, 206.5, 207.3; IR (CH_2Cl_2) ν_{CO} 2011, 1952 (sh), 1949 cm^{-1}; UV (THF) λ_{max} 272 (ϵ 7200), 330 (4800), 395 (sh, 1000) nm; MS *m/z* (rel intensity) 499 (M^+, 47), 384 ($M^+ - 4CO$, 100). Anal. Calcd for $C_{18}H_{16}O_4Ru_2$: C, 43.37; H, 3.24. Found: C, 43.58; H, 3.20.

(*S-3′-*tert*-Butylfulvalene)[*R**-Ru′(CO){P(OCH$_3$)$_3$}][Ru(CO)$_2$] (22a) and (*S**-3′-*tert*-Butylfulvalene)[Ru′(CO)$_2$][*R**,*S**-Ru(CO){P(OCH$_3$)$_3$}] (22b,c).** A solution of **20** (0.5 g, 1.0 mmol) in THF (5 mL) was exposed to $P(OCH_3)_3$ (1.0 mL, 8.5 mmol) and heated to 120 °C for 40 h as in the preparation of **14**. Chromatography of the crude product on activated alumina with toluene−hexanes (1:2) as eluant removed traces of **21**, and subsequent elution with CH_2Cl_2 afforded a mixture of **22a**−**c** (1:1.3:1.3 by ^{1}H NMR) as an orange oil (335 mg, 56%). The mixture was directly converted to the mixture of photoisomers **23a**−**c** which were then separated by HPLC (see below). Separate solutions of **23a** and **23b**,**c** in acetone-d_6 were allowed to stand at room temperature for ∼1 d (until complete conversion was apparent by ^{1}H NMR spectroscopy). Both products were isolated in quantitative yield: **22a** by precipitation from acetone−hexanes, **22b**,**c** by rotary evaporation of solvent. For **22a**: orange powder, mp 148−150 °C; ^{1}H NMR (300 MHz, acetone-d_6) δ 1.26 (s, 9H), 3.50 (d, J = 11.9 Hz, 9H), 4.02 (m, 1H), 4.19 (m, 2H), 4.28 (ddd, J = 4.1, 2.0, 1.8 Hz, 1H), 5.42 (m, 1H), 5.72 (m, 2H); ^{13}C{^{1}H} NMR (acetone-d_6) δ 31.7, 32.0, 52.0 (d, J = 3.0 Hz), 73.8 (d, J = 14.7 Hz), 76.1, 79.3, 79.6, 83.9, 87.5, 89.1, 91.0, 94.2, 122.7; ^{31}P{^{1}H} NMR (acetone-d_6) δ 170.0 (s); IR (CH_2Cl_2) ν_{CO} 1926, 1985 cm^{-1}; UV (THF) λ_{max} 274 (ϵ 12 300), 335 (7200), 418 (1300) nm; MS *m/z* (rel intensity) 595 (M^+, 53), 510 ($M^+ - 3CO$, 100). Anal. Calcd for $C_{20}H_{25}O_6PRu_2$: C, 40.34; H, 4.40. Found: C, 40.63; H, 4.43. For **22b**,**c** (interconverting diastereomers): orange oil; ^{1}H NMR (300 MHz, acetone-d_6, 20 °C) δ 1.24 (s, 18 H), 3.44 (d, J = 12.2 Hz, 18H), 4.06 (br s, 2H), 4.22 (br s, 6H), 5.43 (br s, 4H), 5.70 (dd, J = 2.5, 2.0 Hz, 2H); ^{13}C{^{1}H} NMR (acetone-d_6, −70 °C) δ 31.1, 31.3, 31.4, 31.7, 51.6 (d, J = 4.5 Hz), 67.6 (2 C), 76.1, 76.3, 76.5, 77.2, 77.3, 77.7, 78.0, 78.1, 84.2, 84.8, 86.4, 86.8, 90.9, 91.1, 93.9, 94.0, 125.2, 126.6; ^{31}P{^{1}H} NMR (acetone-d_6, 20 °C) δ 173.5 (s); IR (CH_2Cl_2) ν_{CO} 1982, 1925 cm^{-1}; UV (THF) λ_{max} 273 (ϵ 11 500), 335 (7000), 418 (1200) nm; MS *m/z* (rel intensity) 595 (M^+, 50), 510 ($M^+ - 3CO$, 100). Anal. Calcd for $C_{20}H_{25}O_6PRu_2$: C, 40.34; H, 4.40. Found: C, 40.72; H, 4.29.

(*S-μ_2-η^1:η^5-3′-*tert*-Butylcyclopentadienyl)[*R**-Ru′(CO){P(OCH$_3$)$_3$}]-(μ_2-η^1:η^5-cyclopentadienyl)[Ru(CO)$_2$] (23a) and (*S**-μ_2-η^1:η^5-3′-*tert*-Butylcyclopentadienyl)[Ru′(CO)$_2$](μ_2-η^1:η^5-cyclopentadienyl)[*R**,*S**-Ru(CO){P(OCH$_3$)$_3$}] (23b,c).** A solution of **22a**−**c** (1:1.3:1.3, 84 mg, 0.14 mmol) in THF (50 mL) was irradiated (projector lamp, Variac setting 50 V) at RT for 3 h. Chromatography on activated alumina eluting with Et_2O−hexanes (1:2) gave **23a**−**c** as a colorless oil (1:1.3:1.3, 51 mg, 61%) followed by unreacted **22a**−**c** (30 mg, 36%). The photoisomers were separated by HPLC [CH_2Cl_2−toluene−hexanes (1:8:11), flow rate 5.0 mL min^{-1}, 300 nm monitoring wavelength] to give first **23a** and then **23b**,**c**, which upon removal of solvent were isolated in quantitative yield as a white powder and a colorless oil, respectively. Crystals of **23a** suitable for X-ray crystallography were obtained by cooling a saturated hexanes solution to −20 °C. For **23a**: mp 128−129 °C; ^{1}H NMR (300 MHz, acetone-d_6) δ 1.18 (s, 9H), 3.57 (d, J = 12.0 Hz, 9H), 4.20 (m, 1H), 4.72 (ddd, J = 5.0, 1.8, 1.7 Hz, 1H), 4.83 (m, 1H), 4.88 (m, 1H), 5.20 (m, 1H), 5.48 (m, 1H), 5.53 (m, 1H); ^{13}C{^{1}H} NMR (acetone-d_6) δ 31.4, 32.5, 52.2 (d, J = 3.4 Hz), 78.6, 84.5 (2 C), 90.8, 91.6, 93.3 (d, J = 16.5 Hz), 93.9, 96.2 (d, J = 4.8 Hz), 97.9, 127.6; ^{31}P{^{1}H} NMR (acetone-d_6) δ 165.2 (s); IR (CH_2Cl_2) ν_{CO} 2006, 1946, 1933 (sh) cm^{-1}; UV (THF) λ_{max} 239 (ϵ 3600), 286 (1400) nm; FAB-MS (NBA) 596 ($M^+ + 1$), 567 ($M^+ - CO$). Anal. Calcd for $C_{20}H_{25}O_6PRu_2$: C, 40.34; H, 4.40. Found: C, 40.56; H, 4.31. For **23b**,**c**: ^{1}H NMR (300 MHz, acetone-d_6) δ 1.13 (s, 9H), 1.15 (s, 9H), 3.53 (d, J = 12.1 Hz, 9H), 3.54 (d, J = 12.1 Hz, 9H), 4.33 (dddd, J = 2.3, 1.6, 1.6, 1.5 Hz, 1H), 4.35 (dddd, J = 2.3, 1.6, 1.6, 1.5 Hz, 1 H), 4.63 (dd, J = 2.1, 1.9 Hz, 1H), 4.66 (dddd, J = 4.8, 2.3, 1.6, 1.5 Hz, 1 H), 4.67 (dd, J = 2.2, 1.9 Hz, I H), 4.71 (dddd, J = 4.8, 2.3, 1.6, 1.5 Hz, 1H), 4.85 (dd, J = 1.9, 1.9 Hz, 1H), 4.87 (dd, J = 1.9, 1.9 Hz, 1H), 5.21 (m, 2H), 5.25 (m, 2H), 5.46 (dd, J = 2.2, 1.9 Hz, 1H), 5.48 (dd, J = 2.1, 1.9 Hz, 1H); ^{13}C{^{1}H} NMR (THF-d_8) δ 31.3 (2 C), 32.4, 32.5, 52.2 (d, J = 3.1 Hz), 80.6, 80.7, 87.6, 87.7, 87.8, 87.9, 88.1, 92.1, 92.3, 92.5, 92.7, 93.9, 94.0, 94.6, 94.7, 94.8, 94.9, 95.5, 95.7, 96.0, 97.1, 130.6, 130.7, 203.2, 203.3, 203.9, 204.0, 204.7 (d, J = 26.6 Hz), 204.8 (d, J = 26.1 Hz); ^{31}P{^{1}H} NMR (acetone-d_6) δ 166.3 (s), 166.6 (s); IR (CH_2Cl_2) ν_{CO} 2004, 1943 (br) cm^{-1}; UV (THF) λ_{max} 239 (ϵ 6900), 286 (2800) nm; FAB-MS (NBA) 596 ($M^+ + 1$), 567 ($M^+ - CO$). Anal. Calcd for $C_{20}H_{25}O_6PRu_2$: C, 40.34; H, 4.40. Found: C, 40.72; H, 4.48.

Kinetics of the Thermal Reversions of 2, 15, and 23. In each case, a standard solution of the respective photoisomer (∼9×10^{-4} M) in diglyme (or, in one instance, in decane) was transferred in the glovebox to 1 cm pathlength fused quartz cuvettes which were sealed with Teflon vacuum valves. For the kinetic runs under CO, the solution in the cuvette was degassed on the vacuum line and 1 atm of CO was admitted. Individual isomerizations were performed and monitored at 418 nm over greater than three half-lives at 65, 85, and 99 °C. The temperatures were maintained (<±l °C) using an HP9101A variable temperature cuvette holder attached to an HP89100A temperature controller. Clean first-order kinetics were obeyed at each temperature leading to calculated rate constants with correlation coefficients >0.9999. Application of the Eyring equation to the rate constant data for each compound allowed calculation of the activation parameters cited in Table 6.

(η^5:η^5-Fulvalene)Ru$_2$(CO)$_4$Cl$_2$ from 2. In a typical experiment, a solution of **2** (3 mg, 0.007 mmol) in dioxane-d_8 (0.6 mL) and CCl_4 (0.32 mL) was heated to 80 °C in a sealed NMR tube for 1 h. X-ray quality yellow crystals (2 mg, 66%) of product were deposited over the course of the reaction: mp 200 °C (dec.); ^{1}H NMR (300 MHz, dioxane-d_8) δ 5.36 (ddd, J = 3.3, 2.2, 1.3 Hz, 4H), 5.77 (ddd, J = 3.3, 2.2, 1.3 Hz, 4H); IR (KBr) ν_{CO} 2061, 1996 cm^{-1}. Anal. Calcd for $C_{14}H_8Cl_2O_4Ru_2$: C, 32.76; H, 1.57; Cl, 13.82. Found: C, 32.92; H, 1.67; Cl, 13.40.

(η^5:η^5-Fulvalene)Ru$_2$(CO)$_4$Cl$_2$ from 1. To complex **1** (65 mg, 0.151 mmol) in THF (10 mL) was added solid $Fe(Cl)_3 \cdot 6H_2O$ (79 mg, 0.29 mmol). The mixture was allowed to stir at RT for 28 h and filtered through Celite, and the solvent removed. The resulting orange residue was preadsorbed on Celite and eluted from a silica gel column with CH_2Cl_2−ethyl acetate (5:1) as a narrow yellow band (58 mg, 78%). Spectral data matched those for (η^5:η^5-fulvalene)Ru$_2$(CO)$_4$Cl$_2$.

Thermal Conversion of 2 to 1 in the Presence of ^{13}CO. A solution of **2** (10 mg, 0.02 mmol) in THF (5 mL) in a Pyrex vessel fitted with a Teflon vacuum valve was degassed, the container was evacuated, ^{13}CO (1 atm) was added, and the solution was allowed to stand at RT for 36 h. The solvent was removed from the yellow solution using an N_2 stream. The resulting yellow powder was subjected to mass spectral analysis which revealed the presence of approximately 40% ^{13}CO. The experiment was repeated in an NMR tube containing **2** (20 mg, 0.04 mmol) in THF-d_8 (0.4 mL). ^{13}C NMR spectra taken after 3 and 24 h intervals indicated the absence of label incorporation into unreacted **2** (90% unreacted after 3 h, 30% after 24 h) but significant incorporation into **1**. In a control experiment, the first procedure was repeated starting with **1**. Analysis of the parent ion peak envelope after ^{13}CO exposure showed the absence of ^{13}CO beyond its natural abundance.

Reaction of 2 with P(CH$_3$)$_3$. To a solution of **2** (10 mg, 0.02 mmol) in THF-d_8 (0.4 mL) in an NMR tube was added $P(CH_3)_3$ (∼10 μL, 0.11 mmol). The tube was sealed, and the solution was allowed to stand at RT in the dark. Monitoring by ^{1}H and ^{31}P NMR spectroscopies indicated that, after 21 h, **2** had been consumed to give **25**−**27** (7:3:10). Alternatively, after 3 d at 0 °C only a trace (3%) of **2** remained and the product ratio was 10.5:2:12.5. The tube was opened in the glovebox and pentane was added, and the resulting solution was cooled to generate a brown precipitate containing **25** and **26**. For compound **25**: ^{1}H NMR (300 MHz, THF-d_8) δ 6.08 (m, 2H), 5.83 (m, 2H), 5.67 (m, 2H), 4.77 (m, 2H), 1.27 (d, J = 10.5 Hz, 9H); ^{31}P{^{1}H} NMR (THF-d_8) δ 4.82 (s); IR (THF) ν_{CO} 2017, 1961 cm^{-1}.

Reaction of 13 with P(CH$_3$)$_3$. A solution of **13** (25 mg, 0.05 mmol) in THF (5 mL) was exposed to $P(CH_3)_3$ (∼0.2 mL, 2.4 mmol) and heated to 120 °C for 24 h, as in the published preparation of **26** from **1**.[7d] Crystallization of the crude product from THF−hexanes afforded **26** (16 mg, 79%). The solvent was removed from the mother liquor, and the yellow residue was crystallized from hexanes (−20 °C) to give **27** (11 mg, 60%): yellow crystals, mp 60−61 °C; ^{1}H NMR (300 MHz, acetone-d_6) δ 1.45 (pseudodoublet, J = 6.0 Hz); ^{31}P{^{1}H} NMR (acetone-d_6) δ −3.50; IR (THF) ν_{CO} 1894 (m), 1839 (s) cm^{-1}; MS *m/z* (rel intensity) 386 (M^+, 63), 358 ($M^+ - CO$, 40), 330 ($M^+ - 2CO$, 96), 254 ($M^+ - P(CH_3)_3$, −2CO, 100). Anal. Calcd for $C_{11}H_{27}O_2P_3Ru$: C, 34.29; H, 7.06. Found: C, 34.67; H, 7.25.

Table 7. Summary of Crystal and Data Collection Parameters fo $FvRu_2(CO)_4$ (**1**), (μ_2-η^1:η^5-Cyclopentadienyl)$_2Ru_2(CO)_4$ (**2**), Fv(μ_2-η^1:η^5-cyclopentadienyl)$_2Ru_2(CO)_6$ (**6**), $FvRu_2(CO)_3(HCCH)$ (**8**), and (S*-μ_2-η^1:η^5-3′-*tert*-Butylcyclopentadienyl)[R*-Ru′(CO){$P(OCH_3)_3$}](μ_2-η^1:η^5-cyclopentadienyl)-[$Ru(CO)_2$] (**23a**)

compound	**1**[a]	**2**[a]	**6**[a]	**8**[a]	**23a**[b]
formula	$C_{14}H_8O_4Ru_2$	$C_{14}H_8O_4Ru_2$	$C_{26}H_{16}O_6Ru_4$	$C_{17}H_{10}O_3Ru_2$	$C_{20}H_{25}O_6PRu_2$
mol wt	442.36	442.36	828.69	464.40	594.53
a (Å)	12.7489(5)	7.0874(20)	14.0914(17)	8.0515(10)	18.460(5)
b (Å)	6.9816(5)	8.5705(17)	12.8248(8)	15.0105(19)	9.742(2)
c (Å)	15.8212(12)	12.8038(21)	13.1351(11)	21.8239(32)	13.653(3)
α (deg)		71.909(15)			
β (deg)	112.360(5)	79.752(18)			110.01(2)
γ (deg)		64.418(19)			
V (Å^3)	302.4(3)	665.9(3)	2373.8(6)	2637.6(1.0)	2307.1(9)
Z	4	2	4	2	4
space group	$P2_1/n$	$P1$	$Pca2$ (No. 29)	$\bar{P}1$	$P2_1/c$
D_{calcd}, g cm^{-1}	2.26	2.21	2.31	2.22	1.719
2 θ range (deg)	3−45	3−45	3−45	3−45	3−55
no. of unique reflns[c]	1702	1473	1569	1609	4814
cryst size (mm)	0.12 × 0.25 × 0.35	0.13 × 0.14 × 0.28	0.09 × 0.21 × 0.31	0.14 × 0.27 × 0.36	0.78 × 0.55 × 0.31
no. of variables	182	189	325	222	308
R (%)	1.76	5.73	1.15	1.71	3.90
$R_{w\ (\%)}$	3.20	7.46	1.49	2.91	4.50

[a] For references and footnotes relevant to these structure determinations see refs 43−52 in Hersh, W. H.; Hollander, F. J.; Bergman, R. G. *J. Am. Chem. Soc* **1983**, *105*, 5834. Structure determined by Dr. F. J. Hollander at the UCB CHEXRAY facility on an Enraf-Nonius CAD4 diffractometer. [b] Structure determined by Prof. R. Boese at the Universität Essen-GH on a Nicolet R3 diffractometer. [c] $F^2 > 3\sigma(F^2)$ for all structures except **23a** in which $F^2 > 3.5\sigma(F^2)$.

(η^5:η^5-Fulvalene)$Ru_2(^{13}CO)_4$ (1-^{13}CO). Complex **1** (100 mg) in DME (100 mL) in a 250 mL Pyrex flask was saturated with ^{13}CO and then heated to reflux and irradiated with a broad-band light source for 5 h, while the ^{13}CO atmosphere was regenerated every hour. Removal of the solvent, followed by filtration of the residue through a short column of alumina gave 60% statistically labeled **1** (75 mg), as ascertained by ^{13}C NMR and mass spectral analysis.[51]

X-ray Crystallography. Crystals of **1**, **6**, and **8** were mounted on glass fibers with polycyanoacrylate cement and crystals of **2** and **23a** were sealed in glass capillaries. Crystallographic information for all of the complexes is listed in Table 7. Raw intensity data (Mo Kα radiation, $\omega - 2\theta$ scans) were converted to structure factor amplitudes and their esds by corrections for background, scan speed, and Lorentz and polarization effects. No corrections for crystal decay were necessary. Empirical absorption corrections were applied to the data for **1**, **2**, **6**, and **8**, but not for **23a**. All of the structures were solved by Patterson methods and refined via standard least-squares and Fourier techniques. The positions of all non-hydrogen atoms were refined with anisotropic thermal parameters, and the H atom positions were placed at calculated sites for the final refinement cycles.

For **2**, unit weights were used for the data to avoid unreasonable values for the anisotropic thermal parameters of the ring carbon atoms. The only major features of a difference Fourier map were two peaks of 5.4 and 4.3 e$^-$/Å^3 near Rul and Ru2 which were interpreted as a pair of low-occupancy alternate positions for the two Ru atoms. These features were included in least-squares calculations with fixed B_{iso} (3.0 Å^3) and variable occupancy (refined to 6.5% and 8.1%, respectively). The formation of an additional (polymeric?) species during data collection is implicated by these results, the full interpretation of which will be reported elsewhere.

For **6**, refinement of the two possible enantiomorphic structures was undertaken (all atoms refined with isotropic thermal parameters aganist the 3013 unique data for point group *Pmm*2). All residuals were identical for each of the two structures, implying that both enantiomorphs were present in the sample crystal in equal amounts. All further refinement used the averaged data [$R(I) = 1.4\%$, 1632 data].

The largest peaks in the final difference Fourier maps were 0.22 e$^-$/Å^3 near Rul for **1**, 2.0−0.9 e$^-$/Å^3 near the Ru atoms with no apparent pattern for **2**, 0.32 e$^-$/Å^3 near Rul for **6**, 0.34 e$^-$/Å^3 near Rul for **8**, and 1.07 e$^-$/Å^3 near Rul for **23a**. Selected bond distances and angles are presented in Table 1. For further details of the X-ray structural determinations of **6**, **23a**, and $FvRu_2(CO)_4Cl_2$ see the Supporting Information. The X-ray structural data for complexes **1**, **2**, and **8** are located in the Supplementary Material Sections of ref 7a,c.

Acknowledgment. This paper is dedicated to Professor D. Seebach on the occasion of his 60th birthday. This work was supported by the Director, Office of Energy Research, Office of Basic Energy Sciences, Chemical Sciences Division of the U.S. Department of Energy, under Contract DE-AC03-76SF00098. W.B.T. was the recipient of a W. R. Grace Graduate Fellowship and K.P. of a Feodor Lynen Postdoctoral Fellowship. A.J.M. was a Syntex Predoctoral and an ACS Division of Organic Chemistry Graduate Fellow (sponsored by Rohm and Haas Co.). We thank Johnson Matthey Alfa Aeser for a generous loan of $RuCl_3 \cdot xH_2O$ and Professors R. G. Bergman and C. D Hoff for useful discussions.

Supporting Information Available: Details of the structural determination of **6**, **23a**, and $FvRu_2(CO)_4Cl_2$, including tables of bond lengths and angles, positional and thermal parameters, and additional structural data (37 pages). See any current masthead page for ordering and Internet instructions.

JA9707062